COMMUN. MATH. SCI.
Vol. 12, No. 8, pp. 1379–1407

A COARSE GRAINED STOCHASTIC MULTI-TYPE PARTICLE INTERACTING MODEL FOR TROPICAL CONVECTION: NEAREST NEIGHBOUR INTERACTIONS*

BOUALEM KHOUIDER†

Abstract. Particle interacting systems on a lattice are widely used to model complex physical processes that occur on much smaller scales than the observed phenomenon one wishes to model. However, their full applicability is hindered by the curse of dimensionality so that in most practical applications a mean field equation is derived and used. Unfortunately, the mean field limit does not retain the inherent variability of the microscopic model. Recently, a systematic methodology was developed and used to derive stochastic coarse-grained birth-death processes which are intermediate between the microscopic model and the mean field limit, for the case of the one-type particle-Ising system. Here we consider a stochastic multicloud model for organized tropical convection introduced recently to improve the variability in climate models. Each lattice is either clear sky or occupied by one of three cloud types. In earlier work, local interactions between lattice sites were ignored in order to simplify the coarse graining procedure that leads to a multi-dimensional birth-death process; Changes in probability transitions depend only on changes in the large-scale atmospheric variables. Here the coarse-graining methodology is extended to the case of multi-type particle systems with nearest neighbour interactions and the multi-dimensional birth-death process is derived for this general case. The derivation is carried under the assumption of uniform redistribution of particles within each coarse grained cell given the coarse grained values. Numerical tests show that despite the coarse graining the birth-death process preserves the variability of the microscopic model. Moreover, while the local interactions do not increase considerably the overall variability of the system, they induce a significant shift in the climatology and at the same time boost its intermittency from the build up of coherent patches of cloud clusters that induce long time excursions from the equilibrium state.

Key words. Particle interacting systems, coarse graining, stochastic parametrization, tropical convection, conditional expectation.

AMS subject classifications. 70, 65C05, 65C35, 76.

1. Introduction

Particle interacting systems on a lattice are very useful for studying processes occurring on much smaller scales than those of the observed phenomenon one wants to model. A rigorous theoretical treatment of this subject and a few abstract examples are given in [1]. While the theory is often laid in the very general context, apart from a few exceptions, including the present work, concrete examples with multiple particle species or types are not very abundant. However, the relatively simple case of one-type particle system, known as the Ising model, is widely used in practice [1, 2]; for the Ising model, all the particles are assumed to be identical and each lattice site is either occupied by a particle or is free. It is often represented by an order parameter σ that accordingly takes the values 1 or 0. There is another variant of the Ising model where the model assumes two particle types but each lattice site is always occupied by one particle of either type and never empty. The order parameter takes accordingly the values ± 1.

While it is originally designed for magnetization [2], applications of the Ising model range from the general treatment of the phase transition phenomenon [3] to tropical convection [4, 5, 6] including material science [7, 8], front propagation [9], and

*Received: January 21, 2013; accepted (in revised form): September 23, 2013. Communicated by Eric Venden-Eijnden.

†Department of Mathematics and Statistics, University of Victoria, PO BOX 3045 STN CSC Victoria, B.C., Canada V8W 3P4 (khouider@uvic.ca).

traffic flows [10, 11]. The coupling of this model to a deterministic dynamical system is extensively explored in [12, 13]. See also [14] where more complex stochastic and deterministic dynamics are considered.

For the case of the multi-type particles however very few applications are known to exist and they are fairly recent. They include material science [15], wild fires [16], tropical convection (the topic of the present paper) [17], and pedestrian traffic [18]. The description of the multi-type particle system for the case of tropical convection is given below.

Despite the tremendous improvements in computational resources, today's climate models (GCMs) simulate very poorly rainfall variability in the tropics [19, 20, 21, 22]. It is argued in the discipline literature that improving tropical climate variability will lead to improved long term weather predictions over a few weeks to months, based on documented connections between tropical and midlatitude weather systems [23, 24, 25]. The climate bias in GCMs is believed to be due to the inadequate treatment of clouds and convection processes which occur, in nature, at the sub-grid scale with respect to the climate model grid of 50 to 200 km. Because convection can not be resolved on such grids, GCMs rely on parametrization to represent the bulk effects of convection on the resolved atmospheric flow [26]. Because of their deterministic nature, the traditional cumulus parameterizations used in operational climate models fail to represent the subgrid scale variability associated with convection. Moreover, these parameterizations are not specifically designed to represent the complex mesoscale organized dynamics of tropical convection, which involve interactions between three main cloud types: cumulus congestus clouds with tops below the freezing level (around 5 to 6 km), deep penetrative clouds that reach near the tropopause, and stratiform anvil clouds that trail deep convection in the upper troposphere [27, 28]. Khouider and Majda [29, 30, 31] introduced a multicloud deterministic model parameterization which by design incorporates these interactions between the three cloud types. As such, the deterministic multicloud model is very successful in representing the large scale (wave) variability associated with tropical convection including synoptic scale and planetary/intra-seasonal convectively coupled waves that are notoriously challenging for operational GCMs; this is done in the context of simple models [29, 32, 30, 31, 33, 34] and in the context of an idealized climate model with coarse resolution [35]. A comprehensive review of these results and other recent work on tropical wave dynamics and PDEs is found in [36].

The need for stochastic parametrization in climate models become apparent only recently, namely since the work of Buizza et al. [37]. Since then there were interesting attempts to use a stochastic parameterization for convection in GCMs [38, 39, 40]. It is sought as a systematic way to represent the missing variability in GCMs due to unresolved sub-grid processes [41]. Instead of the static sampling attempted in the previous citations, Majda and Khouider [4] were the first to introduce a Markovian stochastic parameterization for convective inhibition (CIN) based on the Ising model of statistical mechanics. It is further coarse grained to obtain a Markov birth-death process, which is two-way coupled to the large-scale dynamics and which can be integrated into a GCM with very little computational overhead [5]. The stochastic CIN model is used in [5, 6] to improve the wave variability and climate in an otherwise deficient mass-flux like parameterization in the context of a simple one-and-a-half layer toy GCM. Similar stochastic models were also used for statistical analysis of observational data of clouds and convective precipitation [42, 43] and for the parametrization of convective momentum transport [44].

A stochastic version of the stochastic multicloud model is introduced in [17] and utilized recently in [45] and in [46] to improve the convective variability of the deterministic multicloud model. In a recent paper [47], Peters et al. found that the variability of the stochastic multicloud model compares very well with observations. Despite this success, an apparent shortcoming of the stochastic multicloud model in [17] is the neglect of local interactions between lattice sites. In other words, the lattice sites make transitions from one cloud type to another with transition probabilities that depend only on exogenous factors that represent the state of the large scale flow, according to whether the large-scale atmospheric state favours one cloud type or another; the probability transitions do not depend on the particular microscopic configuration of the lattice system. The reason for this simplification is because local interactions prevent a straightforward derivation of a coarse-grained (multi-dimensional) birth-death process that can be cheaply simulated during the time integration of the climate model without any significant computational overhead.

The full applicability of particle interacting systems is hindered by the curse of dimensionality so that in most practical applications a mean field equation is derived and used [48, 18]. Unfortunately, the mean field limit does not retain the intrinsic variability of the stochastic lattice model. A systematic coarse-graining technique that leads to a stochastic birth-death process is developed in [49, 50] for the case of the one particle-type Ising system, when local interactions are present, which nicely approximates the dynamics of the particle interacting system and preserves the convergence to the same mean field equation in the limit of large number of lattice sites and long range interaction potential. This is the model used in [5] and in [6] for tropical convection. A rigorous error analysis for this coarse graining methodology is conducted in [51]. However, the application of this procedure to the multi-type particle system is not straightforward.

The goal of the present paper is to generalize the coarse-graining procedure of [49, 50] to the case of multi-type interacting particles with local interaction dynamics, in the context of the stochastic multi-cloud model for tropical convection [17]. To avoid the long range interaction assumption, which is incompatible with the nearest neighbour potential case (which is more appropriate for atmospheric convection because the underlying physical process, via which clouds can influence each other, such as gravity waves, turbulent mixing, and density currents, have a finite speed of propagation), here we circumvent the Taylor approximation used in [49, 50] by using instead conditional expectations of the microscopic transition rates. More recent coarse-graining work for the case of local or short range interactions using other techniques can be found in [52, 53, 54].

The reminder of the paper is organized as follows. In Section 2, we present the microscopic stochastic multicloud model with local interactions as a multi-type particle interacting system having the Gibbs grand canonical distribution as an equilibrium measure, based on the Ising model framework. The new coarse graining strategy using a mean value approximation of the conditional expectations and the resulting multi-dimensional birth-death process in the case of nearest neighbour interactions are discussed in Section 3. In Section 4, we formally derive the mean field equations and in Section 5 we present a few numerical results to assess the ability of the coarse-grained model to represent the stochastic chaotic dynamics of the multi-type interacting particle system using the mean field limit as a bench mark. A conclusion is given in Section 6.

2. The microscopic multi-type interacting particle cloud model

We consider a two-dimensional lattice of $N = n \times n$ sites overlaying the horizontal computational grid of a climate model (GCM), i.e, the surface of the Earth, for example:

$$\mathcal{L} \equiv \frac{1}{n}\mathbb{Z}^2 \cap [0,1] \times [0,1].$$

The lattice sites are assumed to be 1 to 10 km apart. At any given time t, each lattice site is either occupied by a certain cloud type or it is a clear sky site. We assume the prominence of three cloud types: congestus, deep, and stratiform that are believed to play a central role in the dynamics of organized tropical convective systems [27, 55, 17]; see figure 2.1.

Let X_t be the $\mathbb{R}^N$ vector field that takes values 0,1,2,3 at each lattice site, $i, 0 \leq i \leq N$, according to whether the given site is occupied by a cloud of a certain type or it is a clear sky site at time t.

$$X_t = \begin{cases} 0, & \text{at a clear sky site,} \\ 1, & \text{at congestus site,} \\ 2, & \text{at a deep convection site,} \\ 3, & \text{at a stratiform site.} \end{cases} \tag{2.1}$$

We assume that X_t is a stochastic Markov process on the state space $\Sigma = \{0,1,2,3\}^N$. In the jargon of particle interacting systems, an element X of the state space Σ is called a configuration [1, 49]. In the sequel $\mathcal{L}$ will be referred to as the *microscopic lattice* while Σ will be called the microscopic state space and its elements are called microscopic configurations [49, 50] (figure 2.1).

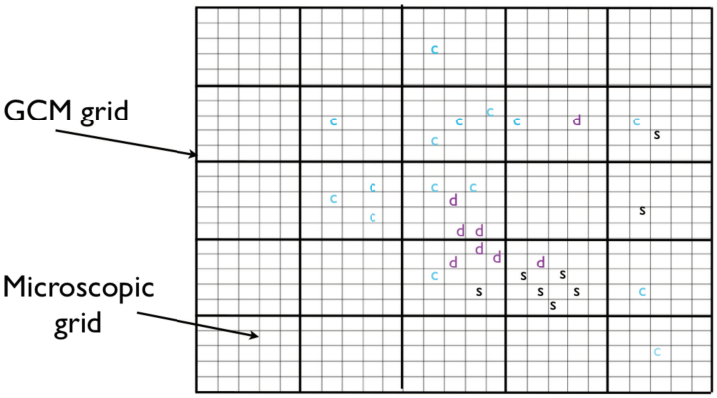

FIG. 2.1. *A microscopic lattice laid on top of a coarse GCM grid. Each lattice is either occupied by a cloud of a certain type (congestus, deep, or stratiform) or it is a clear sky site.*

2.1. The instantaneous infinitesimal transitions and the semi-group generator.

The "Markovian" property is equivalent to assuming that, starting from any given configuration, the process X_t "waits" an exponentially distributed random time S_{kl}^j before it makes a transition at a single site j from state k to l, $0 \leq k, l \leq 3$. This results in a new configuration which is everywhere identical to the

previous one but at the site j where the transition has occurred. Such transformation is called an infinitesimal transition.

According to observations and theory of organized tropical convection [27, 17], only the following seven infinitesimal transitions are assumed to prevail:

$$\begin{aligned}&\text{clear} \longrightarrow \text{congestus}, \quad \text{clear} \longrightarrow \text{deep}, \quad \text{congestus} \longrightarrow \text{deep}, \quad \text{deep} \longrightarrow \text{stratiform},\\ &\text{congestus} \longrightarrow \text{clear}, \quad \text{deep} \longrightarrow \text{clear}, \quad \text{stratiform} \longrightarrow \text{clear}.\end{aligned} \tag{2.2}$$

All other transitions are not allowed, i.e, the associated transition rates are zero. An extensive discussion about the physical motivation behind these assumptions and a more systematic physical derivation of "the stochastic multicloud model" are found in [17]. We skip the details of this discussion here in an attempt to put this model in the more general context where it can be adopted for many other applications, although only the tropical convection example is treated throughout the paper.

More specifically, we have the following. A single transition occurs at a given site j, during the time interval $(t,t+\Delta t)$ (at time s $0\le s\le \Delta t$), if

$$\begin{aligned}X^i_{t+\Delta t} &= \begin{cases} X^i_t, & \text{if } i\neq j,\\ X^j_t+\eta, & \text{if } i=j,\end{cases}\\ \eta &\in \{-3,-2,-1,1,2\}.\end{aligned} \tag{2.3}$$

The value of η in (2.3) is determined by the type of transition that occurs.

$$\begin{aligned}&\eta=1;\ \text{for clear} \longrightarrow \text{congestus}, \text{congestus} \longrightarrow \text{deep, and deep} \longrightarrow \text{stratiform},\\ &\eta=2;\ \text{for clear} \longrightarrow \text{deep},\\ &\eta=-1;\ \text{for congestus} \longrightarrow \text{clear},\\ &\eta=-2;\ \text{for deep} \longrightarrow \text{clear},\\ &\eta=-3;\ \text{for stratiform} \longrightarrow \text{clear}.\end{aligned} \tag{2.4}$$

For simplicity, the infinitesimal transitions in (2.3) are denoted by $X_{t+\Delta t}=X_t+\eta e_j$ where e_j is the jth canonical unit vector of $\mathbb{R}^N$: $e^i_j=\delta_{ij}$. We introduce the indicator function:

$$\mathbb{1}_{\{X^j=k\}} = \begin{cases} 1, & \text{if } X^j=k,\\ 0, & \text{elsewhere.}\end{cases}$$

We denote by $C(X,j,\eta)$ the rate at which the transition $X_{t+\Delta t}=X_t+\eta e_j$ occurs, $j=1,2,\cdots,N$, $\eta=-3,-2,-1,1,2$. If R_{01}, R_{02}, R_{12}, R_{23}, R_{10}, R_{20}, and R_{30} are used to denote the individual rates at which the physical/cloud transitions in (2.2) occur, then the rates $C(X,j,\eta)$ satisfy

$$\begin{aligned}C(X,j,1) &= R^j_{01}\mathbb{1}_{\{X^j_t=0\}}+R^j_{12}\mathbb{1}_{\{X^j_t=1\}}+R^j_{23}\mathbb{1}_{\{X^j_t=2\}},\\ C(X,j,2) &= R^j_{02}\mathbb{1}_{\{X^j_t=0\}},\\ C(X,j,-1) &= R^j_{10}\mathbb{1}_{\{X^j_t=1\}},\\ C(X,j,-2) &= R^j_{20}\mathbb{1}_{\{X^j_t=1\}},\\ C(X,j,-3) &= R^j_{10}\mathbb{1}_{\{X^j_t=0\}}.\end{aligned} \tag{2.5}$$

Here $R^j_{k,l}=R(U,X,j,k,l), 0\le l,k\le 3$ are the prescribed transition rates defined as functions of an external potential U that dictates the dependence of the transition

rates on the large-scale flow variables, the global configuration X, and the particular site j at which the transition occurs.

Forbidden transitions: As noted above, on the physical grounds, only the rates that are listed in (2.5) need to be defined. All other transition rates are set to zero so that a transition permitting conversion of a congestus site to stratiform or a clear to a stratiform, for example, are not allowed. Namely, we have

$$R_{13}=R_{03}=R_{32}=R_{31}=R_{21}=0. \tag{2.6}$$

By definition, the infinitesimal generator of the Markov process X_t is a linear operator defined on the state of bounded functions, from Σ to $\mathbb{R}$ [1]:

$$L_N f(X)=\sum_{j=1}^{N}\sum_{\eta=-3,\eta\neq 0}^{2} C(X,j,\eta)[f(X+\eta e_j)-f(X)],\ \forall f\in L^\infty(\Sigma),\ \forall X\in\Sigma,$$

which defines a semi-group of operators from $L^\infty(\Sigma)$ to $\mathbb{R}$ associated with each realization (or path) of the Markov process X_t: $f\in L^\infty(\Sigma)\longrightarrow E[f(X_t)]$ such that

$$\begin{aligned}\frac{d}{dt}E[f(X_t)]&=E[L_N f(X_t)]\\&=\sum_{j=1}^{N}\sum_{\eta=-3,\eta\neq 0}^{2} E[C(X_t,j,\eta)\{f(X_t+\eta e_j)-f(X_t)\}],\end{aligned} \tag{2.7}$$

where $E[Y]$ denotes the expected value of the random variable Y.

2.2. Invariant measure, detailed balance, and background prior. Consistent with (2.7), a fundamental result from the theory of particle interacting systems states that a probability measure μ on Σ is invariant for the Markov process X_t, if, for all $X\in\Sigma$, it satisfies [1]

$$\int_\Sigma Lf(X)d\mu(X)=0.$$

This is equivalent to

$$\sum_{X\in\Sigma}\sum_{j,\eta} C(X,j,\eta)f(X)d\mu(X)=\sum_{X\in\Sigma}\sum_{j,\eta} C(X-\eta e_j,j,\eta)f(X)d\mu(X-\eta e_j),\quad \forall X\in\Sigma. \tag{2.8}$$

Thus, a sufficient condition for a given probability measure μ to be an invariant measure is given by the *partial detailed balance* relations

$$\sum_{\eta=-3,\eta\neq 0}^{2} C(X,j,\eta)d\mu(X)=\sum_{\eta=-3,\eta\neq 0}^{2} C(X-\eta e_j,j,\eta)d\mu(X-\eta e_j), \tag{2.9}$$

$\forall j=1,2,\cdots,N,\ \forall X\in\Sigma$. This is equivalent to stating that the conditional measure μ given the knowledge of X_t everywhere but at a single site j, is an invariant measure for the restriction of X to the reduced four state space Σ_j: $X_t^i\in\{0,1,2,3\}$ if $i=j$ and X_t^i assumes fixed values for $i\neq j$, $0\leq j\leq N$. Intuitively, this guaranties that at each fixed lattice site j, the random rate at which the reduced process leaves any given state X to go to another state in Σ_j is balanced by the rate at which it enters it from a randomly picked state in Σ_j, without leaving Σ_j. We note in particular that these

balance relations are intermediate between the traditional detailed balance, which requires that at each site $j, 0 \le j \le N$, the effective transition from state $X^j = k$ to state $X^j = k+\nu$, $0 \le k \le 3, -3 \le \nu \le 2$ is balanced by the rate at which it flips back, i.e,

$$C(X,j,\eta)d\mu(X) = C(X-\eta e_j, j, \eta)d\mu(X-\eta e_j),$$

and the more general balance relations in (2.8). However, detailed balance is not possible in our case because of the imposed forbidden transitions in (2.6).

Let $X \in \Sigma$ and $j = 1,2,\cdots,N$ fixed. For simplicity in exposition, we denote by $d\mu(X_j = k)$, the probability of the event that the configuration X is in state k at site j and remains unchanged at other sites, $\forall k = 0,\cdots,3$. Using the relationships in (2.5), the partial detailed balance equations (2.9) become

$$\begin{aligned}
&(R_{02}+R_{01})d\mu(X_j=0) = R_{10}d\mu(X_j=1)+R_{20}d\mu(X_j=2)+R_{30}d\mu(X_j=3),\\
&(R_{12}+R_{10})d\mu(X_j=1) = R_{01}d\mu(X_j=0),\\
&(R_{20}+R_{23})d\mu(X_j=2) = R_{02}d\mu(X_j=0)+R_{12}d\mu(X_j=1),\\
&R_{30}d\mu(X_j=3) = R_{23}d\mu(X_j=2),\ \forall j=1,\cdots,N,\ \forall X\in\Sigma.
\end{aligned} \tag{2.10}$$

Here the superscript j and the dependence on X are dropped out for simplicity in exposition.

Following Katsoulakis et al. [49, 50], we assume that our equilibrium distribution is the compounded Gibbs grand canonical measure given by

$$\mu(dX) \propto \exp(-H(X))P_N(dX), \tag{2.11}$$

where $H(X)$ is the energy Hamiltonian of statistical mechanics that represents the energy of local interactions between neighbouring lattice sites and $P_N(X)$ is a prior distribution given by

$$P_N(dX) = \prod_{i=1}^{N} \rho(dX^i), \quad \rho(X^i = k) = \rho_k,\ k = 0,1,2,3,$$

$\sum_{k=0}^{1} \rho_k = 1$; $(\rho_k)_{k=0,1,2,3}$ is a background prior distribution that depends only on the background state, i.e, the climate model variables that play the role of exogenous factors. Below, we introduce background transition rates, toward which the rates in (2.10) reduce to when the local interactions between lattice sites are ignored, that fully determine the distribution ρ. We note that for the 2-state Ising process treated in [49, 50], without loss of generality, one can always use a uniform background prior and incorporate the external potential U into the Hamiltonian as Katsoulakis et al. [50] did, but here it is a bit complicated.

Following the notation above we set $H_k \equiv H(X/X_j = k)$, and the equations in (2.10) are rewritten as

$$\begin{aligned}
R_{02}+R_{01} &= \frac{\rho_1}{\rho_0}R_{10}e^{H_0-H_1} + \frac{\rho_2}{\rho_0}R_{20}e^{H_0-H_2} + \frac{\rho_3}{\rho_0}R_{30}e^{H_0-H_3},\\
R_{01} &= \frac{\rho_1}{\rho_0}(R_{12}+R_{10})e^{H_0-H_1},\\
R_{02} &= \frac{\rho_2}{\rho_0}(R_{20}+R_{23})e^{H_0-H_2} - \frac{\rho_1}{\rho_0}R_{12}e^{H_0-H_1},
\end{aligned} \tag{2.12}$$

$$R_{30}=\frac{\rho_3}{\rho_2}R_{23}e^{H_2-H_3},\ \forall j=1,\cdots,N,\ \forall X\in\Sigma$$

(Again the dependence of the rates and H_k on the site j is made implicit for ease of notation).

Thus, if for example the "death" rates R_{10}, R_{20}, and R_{30}, the rate of conversion from congestus to deep, R_{12}, and the prior distribution are known, then the three remaining rates are fully determined by the equations in (2.12) provided the Hamiltonian H is also known. To close these equations we need to make a few assumptions on those rates and the Hamiltonian H.

Assumption I: We assume that the "death" rates depend only on the large scale state, i.e, independent of the state X of the system.

$$R_{k0}=\frac{1}{\tau_{k0}}h_{k0},k=1,2,3, \tag{2.13}$$

where τ_{k0} are (arbitrary) background time scales that can be determined from data and h_{k0} are prescribed functions of the external potential U. For simplicity in exposition, the dependence of h_{kl} on U is not written explicitly.

Assumption II: The rate of conversion of congestus to deep is assumed to be proportional to the exponential energy difference between "deep" and "congestus" states.

$$R_{12}=\frac{1}{\tau_{12}}h_{12}(U)e^{H_1-H_2}. \tag{2.14}$$

Here again τ_{12} is a background time scale of creation of deep from congestus. Note that the dependence of R_{12} on the energy difference is such that $H_1-H_2>0$ implies the rate of conversion from congestus to deep is amplified (exponentially) if the targeted state has a lower energy level. As we will see below, the same is true for the remaining birth rates although they are systematically derived from the partial balance equation (2.9) or equivalently (2.12).

The background prior distribution: To construct a background prior distribution, we introduce the background transition rates

$$\tilde{R}_{kl}=\frac{h_{kl}}{\tau_{kl}},\quad k,l=0,1,2,3, \tag{2.15}$$

where τ_{kl} are some background time scales and h_{kl} are the exogenous factors that depend on the large-scale (climate model) variables U.

We define ρ as the equilibrium distribution, solution of (2.12) when the Hamiltonian is zero, i.e, when local interactions are ignored. We have [17]

$$\begin{pmatrix}\rho_0\\ \rho_1\\ \rho_2\\ \rho_3\end{pmatrix}=\frac{1}{Z}\begin{pmatrix}1\\ \frac{\tilde{R}_{01}}{\tilde{R}_{12}+\tilde{R}_{10}}\\ \left(\tilde{R}_{02}+\frac{\tilde{R}_{01}\tilde{R}_{12}}{\tilde{R}_{12}+\tilde{R}_{10}}\right)/(\tilde{R}_{23}+\tilde{R}_{20})\\ \frac{\tilde{R}_{23}}{\tilde{R}_{30}}\left(\tilde{R}_{02}+\frac{\tilde{R}_{01}\tilde{R}_{12}}{\tilde{R}_{12}+\tilde{R}_{10}}\right)/(\tilde{R}_{23}+\tilde{R}_{20})\end{pmatrix}. \tag{2.16}$$

Thus, given the death rates and the rate of conversion of congestus to deep, as by assumptions I and II, the dynamical process having the Gibbs canonical equilibrium

measure given in (2.11) is uniquely determined in terms of the Hamiltonian H and the background rates $\tilde{R}_{kl}$. We have

$$\begin{aligned}
&R_{k0} = \tilde{R}_{k0}, \quad k = 1,2,3,\\
&R_{12} = \tilde{R}_{12} e^{H_1 - H_2},\\
&R_{01} = (\tilde{R}_{12} + \tilde{R}_{10}) \frac{\rho_1}{\rho_0} e^{H_0 - H_1} = \tilde{R}_{01} e^{H_0 - H_1},\\
&R_{02} = \frac{1}{\rho_0}(\rho_2 \tilde{R}_{20} - \rho_1 \tilde{R}_{12}) e^{H_0 - H_2} + \frac{\rho_3}{\rho_0} \tilde{R}_{30} e^{H_0 - H_3},\\
&R_{23} = \frac{\rho_3}{\rho_2} \tilde{R}_{30} e^{H_2 - H_3} = \tilde{R}_{23} e^{H_2 - H_3}.
\end{aligned} \tag{2.17}$$

In order to guarantee that the rate R_{02} is non negative, a physical constraint must be imposed on the above relationships. Simple calculation shows that

$$R_{02} \geq 0 \Longleftrightarrow e^{H_2 - H_3} \geq 1 - \frac{\rho_0}{\rho_2} \frac{\tilde{R}_{02}}{\tilde{R}_{23}}.$$

This suggests the following constraint on the Hamiltonian:

$$\min_{X \in \Sigma} e^{H_2(X) - H_3(X)} \geq 1 - \frac{\rho_0}{\rho_2} \frac{\tilde{R}_{02}}{\tilde{R}_{23}}. \tag{2.18}$$

Given the background prior and background transition rates, this in fact imposes a constraint of the interaction potential that prevents the local interactions from severely limiting the rate at which deep convective clouds are converted into stratiform clouds, especially, when $\rho_2 \tilde{R}_{23} > \rho_0 \tilde{R}_{02}$, i.e, when the background rate of conversion of deep to stratiform is larger than the background rate of birth of deep convective clouds. This is in agreement with the general idea that if deep convective clouds have the tendency of being converted to stratiform anvils with a high probability, then the power of local interactions to reduce this tendency is limited.

2.3. The microscopic Hamiltonian and the nearest neighbour interaction matrix. Let $J_{11}(|i-j|)$, $J_{22}(|i-j|)$, $J_{33}(|i-j|)$, $J_{12}(|i-j|)$, $J_{13}(|i-j|)$, and $J_{23}(|i-j|)$ be non-negative functions that depend only on the distance $|i-j|$ between the two lattice sites i, j. This sequence of functions defines the *matrix of microscopic interaction potentials* between neighbouring sites depending on their respective cloudy states, congestus, deep, or stratiform clouds, respectively. In this paper we assume nearest neighbour interactions to be more important and restrict the support of the interaction functions to the size of one microscopic site. Accordingly we set

$$J_{kl}(|i-j|) = \begin{cases} J^0_{kl} & \text{if } |i-j| \leq 1, i \neq j, \\ 0, & \text{otherwise.} \end{cases} \tag{2.19}$$

Here J^0_{kl} are constants defining the strength of the interactions and $|.|$ is some adequate norm defined on the lattice. For the examples of the L_p and L_∞ distance norms, defined, respectively, by $|r-j|_p = (|r_x - j_x|^p + |r_y - j_y|^p)^{1/p}$ and $|r-j|_\infty = \max(|r_x - j_x|, |r_y - j_y|)$, we have: in the first case, each site j on the 2d lattice has exactly four nearest neighbours, north, south, east, and west, denoted by j^n, j^s, j^e, and j^w, respectively, while in the latter, each site has 8 neighbours: j^n, j^{ne}, j^e, j^w, j^{nw}, j^s, j^{se}, and j^{sw}; see figure 2.2.

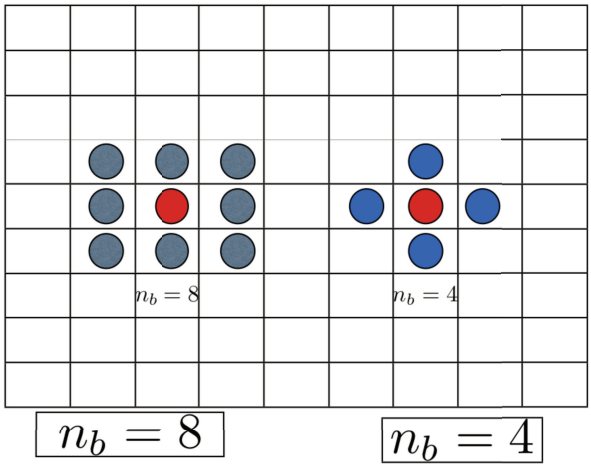

FIG. 2.2. *Configuration of a microscopic site in red with its nearest neighbours. Left* $n_b = 8$ *and right* $n_b = 4$.

Let

$$E_{k,l}(X) = -\sum_{i,j=1, i\neq j}^{N} J_{k,l}(|i-j|)\mathbb{1}_{\{X^i=k\}}\mathbb{1}_{\{X^j=l\}}, 1 \leq k \leq l \leq 3. \tag{2.20}$$

The (total) Hamiltonian energy is then given by

$$H(X,U) = \sum_{k=1}^{3}\sum_{l=k}^{3} E_{k,l}(X). \tag{2.21}$$

Note that the Hamiltonian does not depend on the external large scale factors as this dependence is automatically incorporated into the background transition rates and into the prior distribution. While E_{11}, E_{22}, and E_{33} represent the individual energies associated with each cloud type, $E_{k,l}, k < l$ represent cross correlation contributions. It is important to establish some guidelines or intuitive rules about the relative importance of the components of H, based on observation and/or numerical simulation of self-organization of cloud types. According to the intuition that congestus clouds are more chaotic than both deep and stratiform, that deep clouds and noisier than stratiform, and that clouds of the same type will tend to clump together, one may assume

$$\liminf |E_{3,3}| < \liminf |E_{2,2}| < \liminf |E_{1,1}| \text{ and } \liminf E_{k,l} > \liminf E_{k,k}, l \neq k.$$

However, a systematic quantification of the interaction matrix $J_0 = [J_0(k,l)]$ is needed and will be conducted in the future based on detailed LES simulations and/or in situ observations.

Using (2.20) and (2.21), we can derive closed formulae for the energy differences in (2.17).

$$(H_0 - H_1)_j = \sum_{i=1, i\neq j}^{N} J_{11}(|i-j|)\mathbb{1}_{\{X^i=1\}} + J_{1,2}(|i-j|)\mathbb{1}_{\{X^i=2\}} + J_{1,3}(|i-j|)\mathbb{1}_{\{X^i=3\}},$$

$$(H_0-H_2)_j=\sum_{i=1,i\neq j}^{N} J_{22}(|i-j|)\mathbb{1}_{\{X^i=2\}}+J_{1,2}(|i-j|)\mathbb{1}_{\{X^i=1\}}+J_{2,3}(|i-j|)\mathbb{1}_{\{X^i=3\}},$$

$$(H_0-H_3)_j=\sum_{i=1,i\neq j}^{N} J_{33}(|i-j|)\mathbb{1}_{\{X^i=3\}}+J_{1,3}(|i-j|)\mathbb{1}_{\{X^i=1\}}+J_{2,3}(|i-j|)\mathbb{1}_{\{X^i=2\}},$$

$$\begin{aligned}(H_1-H_2)_j=&\sum_{i=1,i\neq j}^{N} J_{22}(|i-j|)\mathbb{1}_{\{X^i=2\}}-J_{11}(|i-j|)\mathbb{1}_{\{X^i=1\}}+J_{1,2}(|i-j|)\times\\&\left(\mathbb{1}_{\{X^i=1\}}-\mathbb{1}_{\{X^i=2\}}\right)-J_{1,3}(|i-j|)\mathbb{1}_{\{X^i=3\}}+J_{2,3}(|i-j|)\mathbb{1}_{\{X^i=3\}},\end{aligned}\tag{2.22}$$

$$\begin{aligned}(H_2-H_3)_j=&\sum_{i=1,i\neq j}^{N} J_{33}(|i-j|)\mathbb{1}_{\{X^i=3\}}-J_{22}(|i-j|)\mathbb{1}_{\{X^i=2\}}-J_{1,2}(|i-j|)\mathbb{1}_{\{X^i=1\}}\\&+J_{1,3}(|i-j|)\mathbb{1}_{\{X^i=1\}}+J_{2,3}(|i-j|)\left(\mathbb{1}_{\{X^i=2\}}-\mathbb{1}_{\{X^i=3\}}\right).\end{aligned}$$

Notation: If we adopt the notation

$$\Delta^k H_j=H(X/X^j=k)-H(X/X^j=0)\equiv H_k-H_0,\quad k=1,2,3,$$

then we obtain the systematic relations

$$(H_0-H_k)_j=-\Delta^k H_j, k=1,2,3$$

and

$$H_2-H_3=(\Delta^2-\Delta^3)H_j,\quad H_1-H_2=(\Delta^1-\Delta^2)H_j,$$

so that in practice only the quantities $\Delta^k H_j$ need to be obtained.

This completes the description of the (microscopic) stochastic multicloud model with nearest neighbour interactions, which can readily be coupled to a climate model [17]. However, this is computationally impractical given the high dimensionality of the system. The next task is to derive a systematic coarse grained stochastic process which preserves all the desired dynamical features of the microscopic system but is computationally cheap. In fact, the coarse grained process derived below is in essence a family of multi-dimensional birth-death processes with immigration, representing the stochastic dynamics of the cloud area fractions within each GCM grid box, which can then be directly coupled to the GCM's cumulus parameterization in lieu of otherwise fixed or deterministically diagnosed values.

3. The coarse-grained process

We introduce the coarse lattice [49]

$$\mathcal{L}^c\equiv\frac{1}{m}\mathbb{Z}^2\cap[0,1]\times[0,1],$$

where m is a positive integer such that $n=mq$, $q\geq 1$, and $n\times n$ is the number of microscopic sites, the size of the fine lattice $\mathcal{L}$. The total number of coarse sites $M=m\times m$ satisfies $N=q^2M$ and $\mathcal{L}^c\subset\mathcal{L}$. Each coarse site $j, j=1,\cdots,M$, corresponds to a coarse cell D_j which contains exactly q^2 microscopic sites belonging to the fine lattice $\mathcal{L}$ so that

$$\mathcal{L}=\bigcup_{j=1}^{M} D_j.$$

$\mathcal{L}^c$ can be thought of as a horizontal slice of the GCM grid and each D_j is a horizontal slice of one GCM grid box.

We consider the coarse grained stochastic process $\bar{X}_t$ defined as the "three-dimensional vector-field" that takes values on the coarse lattice $\mathcal{L}^c$ constructed directly and consistently from the microscopic process X_t as follows:

$$\bar{X}_t^j = (N_1, N_2, N_3)_t^j,\ j = 1, \cdots, N,$$

where

$$N_k^j = \sum_{i \in D_j} \mathbb{1}_{\{X_t^i = k\}},\quad k = 1,2,3$$

represent, respectively, the number of microscopic sites, within the coarse cell D_j, that are congestus, deep, or stratiform. Here $\bar{X}_t$ is a Markov process on the state space

$$\Sigma^c = \left\{\{0,1,2,\cdots,q^2\} \times \{0,1,2,\cdots,q^2\} \times \{0,1,2,\cdots,q^2\}\right\}^M.$$

The cloud area fractions of congestus, deep, and stratiform cloud types are obtained by dividing N_k by the number of sites contained in each coarse cell D_j:

$$\sigma_c^j = \frac{1}{q^2} N_1,\quad \sigma_d^j = \frac{1}{q^2} N_2,\quad \sigma_s^j = \frac{1}{q^2} N_3^j. \tag{3.1}$$

We introduce the coarse-graining function F defined from Σ to Σ^c by [49, 50]

$$F(X)^j = \bar{X}^j = (N_1, N_2, N_3)^j. \tag{3.2}$$

We recall that $f \longmapsto Ef(X_t)$ is the semi-group of the Markov process X_t if it satisfies (2.7).

Following [50], the coarse graining procedure starts by setting $f(X) = \bar{f}(F(X))$ in (2.7), where F is the coarse-graining function given in (3.2) and $\bar{f}$ is a test function in $L^\infty(\Sigma^c)$. This yields

$$\frac{d}{dt} E\bar{f}(\bar{X}_t) = E \sum_{\eta=-3, \eta \neq 0}^{2} \sum_{i=1}^{M} \left[\sum_{j \in D_i} C(X_t, j, \eta) f(X_t + \eta e_j) - \left(\sum_{j \in D_i} C(X_t, j, \eta) \right) \bar{f}(\bar{X}_t) \right]. \tag{3.3}$$

We now need to express the factors $f(X_t + \eta e_j)$ in terms of $\bar{f}(\bar{X}_t + \bar{a}_i)$, where $\bar{a}_i$ is some perturbation of $\bar{X}_t$ that involves changes only within the coarse cell D_i, i.e, a single coarse site.

We introduce the family of three unit vectors defined on Σ^c:

$$\text{For } i' = 1,2,\cdots,M,\ \ (\bar{e}_i^k)^{i'} = \begin{cases} (\delta_{1k}, \delta_{2k}, \delta_{3k}), & \text{if } i' = i, \\ (0,0,0), & \text{elsewhere,} \end{cases} \tag{3.4}$$

$k = 1,2,3$. We fix $i,\ 1 \leq i \leq M$ and let $j,\ 1 \leq j \leq N$ be an arbitrary microscopic site

contained in D_i. We have

$$f(X_t+\eta e_j)=\begin{cases} \bar{f}(\bar{X}_t-\bar{e}_i^3) & \text{if } \eta=-3\text{: death of one stratiform,}\\ \bar{f}(\bar{X}_t-\bar{e}_i^2), & \text{if } \eta=-2\text{: death of one deep,}\\ \bar{f}(\bar{X}_t-\bar{e}_i^1), & \text{if } \eta=-1\text{: death of one congestus,}\\ \bar{f}(\bar{X}_t+\bar{e}_i^1), & \text{if } \eta=1\text{: birth of a congestus,}\\ \bar{f}(\bar{X}_t+\bar{e}_i^2-\bar{e}_i^1), & \text{if } \eta=1\text{: conversion of a congestus to a deep,}\\ \bar{f}(\bar{X}_t+\bar{e}_i^3-\bar{e}_i^2), & \text{if } \eta=1\text{: conversion of a deep to a stratiform,}\\ \bar{f}(\bar{X}_t+\bar{e}_i^2), & \text{if } \eta=2\text{: birth of a deep,}\end{cases} \tag{3.5}$$

covering all the microscopic infinitesimal transitions in (2.4). Equation 3.3 then becomes

$$\frac{d}{dt}E\bar{f}(\bar{X}_t)=E\sum_{i=1}^{M}\sum_{\tilde{R}_{kl}\neq 0}\left(\sum_{j\in D_i}R_{kl}^j\mathbb{1}_{\{X_t^j=k\}}\right)\left[\bar{f}(\bar{X}_t+\bar{e}_i^l-\bar{e}_i^k)-\bar{f}(\bar{X}_t)\right], \tag{3.6}$$

where $\bar{e}_i^0$ is the zero vector. According to the conditional expectation formula ($E[X]=E[E[X/Y]]$, e.g., [56]), this equation is viewed as the semi-group formulation of the coarse-grained Markov process which is defined at each coarse cell D_i, $\bar{X}_t^i:=\bar{X}_t(D_i)$, as a multi-dimensional birth-death process with immigration [57] whose birth, death, and immigration rates are given by the conditional expectations:

$$\begin{aligned}
&\bar{R}_{0k}^i\equiv E\left[\sum_{j\in D_i}R_{0k}^j\mathbb{1}_{\{X_t^j=0\}}/\bar{X}_t^i\right], k=1,2\text{: Birth of one congestus or one deep, resp.,}\\
&\bar{R}_{k0}^i\equiv E\left[\sum_{j\in D_i}R_{k0}^j\mathbb{1}_{\{X_t^j=k\}}/\bar{X}_t^i\right], k=1,2,3\text{: Death rates,}\\
&\bar{R}_{12}^i\equiv E\left[\sum_{j\in D_i}R_{12}^j\mathbb{1}_{\{X_t^j=1\}}/\bar{X}_t^i\right]\text{: Conversion of one congestus to one deep,}\\
&\bar{R}_{23}^i\equiv E\left[\sum_{j\in D_i}R_{23}^j\mathbb{1}_{\{X_t^j=0\}}/\bar{X}_t^i\right]\text{: Conversion of one deep to one stratiform.}
\end{aligned} \tag{3.7}$$

We obtain

$$\begin{aligned}
\frac{d}{dt}E\bar{f}(\bar{X}_t)=E\sum_{i=1}^{M}&\bar{R}_{30}^i\left[\bar{f}(\bar{X}_t-\bar{e}_i^3)-\bar{f}(\bar{X}_t)\right]\\
&+\bar{R}_{20}^i\left[\bar{f}(\bar{X}_t-\bar{e}_i^2)-\bar{f}(\bar{X}_t)\right]+\bar{R}_{10}^i\left[\bar{f}(\bar{X}_t-\bar{e}_i^1)-\bar{f}(\bar{X}_t)\right]\\
&+\bar{R}_{01}^i\left[\bar{f}(\bar{X}_t+\bar{e}_i^1)-\bar{f}(\bar{X}_t)\right]+\bar{R}_{12}^i\left[\bar{f}(\bar{X}_t+\bar{e}_i^2-\bar{e}_i^1)-\bar{f}(\bar{X}_t)\right]\\
&+\bar{R}_{23}^i\left[\bar{f}(\bar{X}_t+\bar{e}_i^3-\bar{e}_i^2)-\bar{f}(\bar{X}_t)\right]+\bar{R}_{02}^i\left[\bar{f}(\bar{X}_t+\bar{e}_i^2)-\bar{f}(\bar{X}_t)\right],
\end{aligned} \tag{3.8}$$

where the expectations are now taking on the probability space of the coarse configurations $\bar{X}_t\in\Sigma_c$. Because the microscopic (individual) decay rates are assumed to be independent of the microscopic configuration (2.13), the coarse-grained death rates are completely determined from the knowledge of the coarse-grained configuration $\bar{X}_t$.

We have from (3.7)

$$\boxed{\bar{R}_{k0} = \frac{1}{\tau_{k0}} h_{k0}(U) N_t^k, k = 1,2,3.} \tag{3.9}$$

The remaining task is to derive appropriate approximations for the birth and immigration rates in terms of the coarse-grained configuration $\bar{X}_t$.

While the conditional expectations can be expressed explicitly in terms of $\bar{X}_t$, the resulting formula may be very complicated and computationally expensive. Moreover, the coarse grained process resulting from the exact computation of these "integrals" may not be necessarily formulated in terms of a coarse-grained Hamiltonian having a Gibbs canonical measure as its equilibrium distribution, a highly desired feature because it facilitates the theoretical knowledge of the equilibrium distribution. Thus, instead of computing exactly or using highly accurate quadrature formulae to compute the conditional expectations in (3.7), here we use (partial) detailed balance with respect to an assumed Gibbs equilibrium measure for the coarse grained process as a design principle to derive approximate values for the coarse-grained transition rates in (3.7).

3.1. Coarse-grained Gibbs equilibrium measure and detailed balance. Let $\bar{X}_t^i = (N_t^{1,i}, N_t^{2,i}, N_t^{3,i})$ be the coarse grained process and $\bar{a}_i^\eta, 1 \le \eta \le 7$ be the perturbations of $\bar{X}_t$ that are associated with each one of the seven (allowed) infinitesimal transitions of the coarse grained process in (3.7). Here the index i refers to a coarse cell D_i, $1 \le i \le M$. For simplicity, we denote by $\bar{C}(\bar{X}_t, \eta, i)$, $1 \le \eta \le 7$ the infinitesimal transition rates of $\bar{X}_t$. Each transition rate is associated with a specific perturbation of the process so that $\text{Prob}\{\bar{X}_{t+\Delta t} = \bar{X}_t + a_\nu^i\} = \bar{C}(\bar{X}_t, \eta, i)\Delta t$. We have

$$\begin{aligned}
&\bar{C}(\bar{X}_t, k, i) = \bar{R}_{k0}^i, && \bar{a}_k^i = -\bar{e}_i^k, \quad k = 1,2,3 \text{ (the death rates)},\\
&\bar{C}(\bar{X}_t, k, i) = \bar{R}_{0,k-3}^i, && \bar{a}_k^i = \bar{e}_i^{k-3}, \quad k = 4,5 \text{ (the birth rates)},\\
&\bar{C}(\bar{X}_t, 6, i) = \bar{R}_{12}^i, && \bar{a}_6^i = \bar{e}_i^2 - \bar{e}_i^1, \text{ (immigration from congestus to deep)},\\
&\bar{C}(\bar{X}_t, 7, i) = \bar{R}_{23}^i, && \bar{a}_7^i = \bar{e}_i^3 - \bar{e}_i^2, \text{ (immigration from deep to stratiform)}.
\end{aligned} \tag{3.10}$$

We require similar semi-detailed balance relations as for the microscopic process in (2.9) to ensure that the coarse-grained measure $\bar{\mu}$ is an equilibrium measure, i.e,

$$\sum_{\bar{X} \in \Sigma^c} \sum_{i=1}^{M} \sum_{\eta=1}^{7} \bar{C}(\bar{X}_t, \eta, i) \bar{\mu}(\bar{X}) \left[\bar{f}(\bar{X}_t + \bar{a}_\eta^i) - \bar{f}(\bar{X}_t) \right] = 0.$$

Local equilibrium on each coarse cell (i.e, partial detailed balance) then requires

$$\sum_{\eta=1}^{7} \bar{C}(\bar{X}_t, \eta, i) \bar{\mu}(\bar{X}) \left[\bar{f}(\bar{X}_t + \bar{a}_\eta^i) - \bar{f}(\bar{X}_t) \right] = 0, \ \forall \bar{X} \in \Sigma^c, \ \forall i = 1,2,\cdots,M,$$

where the transition rates and elementary perturbations $\bar{a}_i$ are given in (3.10). This is indeed equivalent to setting balance relations between birth, death, and immigration transitions for each cloud type and each coarse cell $D_i, i = 1,\cdots,M$:

$$\begin{aligned}
&\left[\bar{R}_{12}^i(\bar{X}_t + e^1) + \bar{R}_{10}^i(\bar{X}_t + e^1) \right] \bar{\mu}(\bar{X}_t + e^1) = \bar{R}_{01}^i(\bar{X}_t) \bar{\mu}(\bar{X}_t),\\
&\left[\bar{R}_{20}^i(\bar{X}_t + e^2) + \bar{R}_{23}^i(\bar{X}_t + e^2) \right] \bar{\mu}(\bar{X}_t + e^2) = \bar{R}_{02}^i(\bar{X}_t) \bar{\mu}(\bar{X}_t) + \bar{R}_{12}^i(\bar{X}_t + \bar{e}^1) \bar{\mu}(\bar{X}_t + \bar{e}^1),
\end{aligned}$$

$$\bar{R}^i_{30}(\bar{X}_t+\bar{e}^3)\bar{\mu}(\bar{X}_t+\bar{e}^3)=\bar{R}^i_{23}(\bar{X}_t+\bar{e}^2)\bar{\mu}(\bar{X}_t+\bar{e}^2), \tag{3.11}$$

which could be easily surmised from (2.10).

As in the microscopic case, we assume that $\bar{\mu}$ is a Gibbs canonical equilibrium measure:

$$\bar{\mu}(d\bar{X})\propto e^{-\bar{H}(\bar{X},U)}\bar{P}^Q_M(d\bar{X}), \tag{3.12}$$

where $\bar{H}$ is a coarse grained Hamiltonian to be determined (below) and $\bar{P}^Q_M$ is the coarse-grained prior distribution:

$$\bar{P}^Q_M(d\bar{X})=\prod_{j=1}^{M}\bar{\rho}_Q(d\bar{X}_j), \tag{3.13}$$

$$\bar{\rho}_Q(N^1_j=k_1,N^2_j=k_2,N^3_j=k_3)=\frac{Q!}{k_1!\ k_2!\ k_3!\ k_0!}\rho_1^{k_1}\rho_2^{k_2}\rho_3^{k_3}\rho_0^{k_0},\ j=1,\cdots,M,$$

where $k_0=Q-k_1-k_2-k_3$. The coarse grained Hamiltonian $\bar{H}$ will be constructed based on an approximation of some sort of the microscopic Hamiltonian introduced above so that the dynamics and equilibrium measure of the coarse grained Hamiltonian are somewhat similar to the microscopic dynamics: $\bar{H}(\bar{X})\approx H(X)$ if $F(X)=\bar{X}$.

For simplicity in exposition, we introduce the notation

$$\bar{H}_k(\bar{X},i):=\bar{H}(\bar{X}_t+e^k_i),\ k=1,2,3.$$

Then, we obtain the following equations for the coarse grained birth and immigration rates, in terms of the coarse-grained death rates in (3.9):

$$\begin{aligned}
\bar{R}^i_{23}(\bar{X}+\bar{e}^2_i)\bar{P}^Q_M(\bar{X}+\bar{e}^2_i)=&\bar{R}^i_{30}(\bar{X}+\bar{e}^3_i)\bar{P}^Q_M(\bar{X}+\bar{e}^3_i)e^{\bar{H}_2(\bar{X},i)-\bar{H}_3(\bar{X},i)}\\
=&\frac{h_{30}}{\tau_{30}}(N^3_t+1)\bar{P}^Q_M(\bar{X}+\bar{e}^3_i)e^{\bar{H}_2(\bar{X})-\bar{H}_3(\bar{X},i)},\\
\bar{R}^i_{02}(\bar{X})\bar{P}^Q_M(\bar{X})=&-\bar{R}^i_{12}(\bar{X}+e^1_i)\bar{P}^Q_M(\bar{X}+\bar{e}^1_i)e^{\bar{H}(\bar{X})-\bar{H}_1(\bar{X},i)}\\
&+\left[\bar{R}^i_{20}(\bar{X}+\bar{e}^2_i)+\bar{R}^i_{23}(\bar{X}+\bar{e}^2_i)\right]\bar{P}^Q_M(\bar{X}+\bar{e}^2_i)e^{\bar{H}(\bar{X})-\bar{H}_2(\bar{X},i)},\\
\left[\bar{R}^i_{01}(\bar{X})+\bar{R}^i_{02}(\bar{X})\right]\bar{P}^Q_M(\bar{X})=&\bar{R}^i_{10}(\bar{X}+\bar{e}^1_i)\bar{P}^Q_M(\bar{X}+\bar{e}^1_i)e^{\bar{H}(\bar{X})-\bar{H}_1(\bar{X},i)}\\
&+\left[\bar{R}^i_{20}(\bar{X}+\bar{e}^2_i)+\bar{R}^i_{23}(\bar{X}+\bar{e}^2_i)\right]\bar{P}^Q_M(\bar{X}+\bar{e}^2_i)e^{\bar{H}(\bar{X})-\bar{H}_2(\bar{X},i)}\\
=&\bar{R}^i_{10}(\bar{X}+\bar{e}^1_i)\bar{P}^Q_M(\bar{X}+\bar{e}^1_i)e^{\bar{H}(\bar{X})-\bar{H}_1(\bar{X},i)}\\
&+\bar{R}^i_{20}(\bar{X}+\bar{e}^2_i)\bar{P}^Q_M(\bar{X}+\bar{e}^2_i)e^{\bar{H}(\bar{X})-\bar{H}_2(\bar{X},i)}\\
&+\bar{R}^i_{30}(\bar{X}+\bar{e}^3_i)\bar{P}^Q_M(\bar{X}+\bar{e}^3_i)e^{\bar{H}(\bar{X})-\bar{H}_3(\bar{X},i)}.
\end{aligned} \tag{3.14}$$

These are three equations with four unknowns $(\bar{R}^i_{01},\bar{R}^i_{02},\bar{R}^i_{12},\bar{R}^i_{23})$.

A sensible solution to this underdetermined system can be obtained by fixing an "approximate" value for $\bar{R}^i_{12}$, according to (2.17), and then solve for the remaining unknowns. Let $\bar{X}^i=(N^1_i,N^2_i,N^3_i,N^4_i)$ where $N^k,k=0,1,2,3,\cdots i=1,\cdots,M$ are the numbers of respectively clear sky, congestus, deep, and stratiform sites within the coarse cell D_i. We have $N^0_i=Q-N^1_i-N^2_i-N^3_i$, where $Q=q^2$ is the number of microscopic sites within each coarse cell D_i.

Given $\bar{H}(\bar{X})$, we set

$$\bar{R}^i_{12}(\bar{X}+e^1_i)=\frac{h_{12}}{\tau_{12}}(N^1+1)e^{\bar{H}_1(\bar{X},i)-\bar{H}_2(\bar{X},i)}, \tag{3.15}$$

so that

$$\bar{R}^i_{12}(\bar{X}+e^1_i)e^{\bar{H}(\bar{X})-\bar{H}_1(\bar{X},i)}=\frac{1}{\tau_{12}}h_{12}(N^1+1)e^{\bar{H}(\bar{X})-\bar{H}_2(\bar{X},i)}$$

and

$$\bar{R}^i_{12}(\bar{X})=N^1_i\frac{h_{12}}{\tau_{12}}e^{\bar{H}(\bar{X})-\bar{H}(\bar{X}-\bar{e}^1_i+\bar{e}^2_i)}.$$

Let

$$\Delta^k_i H(\bar{H}):=\bar{H}_k(\bar{X},i)-\bar{H}(\bar{X}).$$

We have

$$\boxed{\bar{R}^i_{12}(\bar{X})=\frac{N^1_i}{\tau_{12}}h_{12}e^{(\Delta^1_i-\Delta^2_i)\bar{H}(\bar{X}-\bar{e}^1_i)}.} \tag{3.16}$$

Before we derive the remaining transition rates, let us note that the coarse grained prior in (3.13) satisfies

$$\frac{P^Q_M(\bar{X}+e^k)}{P^Q_M(\bar{X})}=\frac{\rho_k}{\rho_0}\frac{N^0_i}{N^k_i}.$$

Then, combining (3.9), (3.13), (3.14), and (3.15) yields

$$\bar{R}^i_{23}(\bar{X}+\bar{e}^2_i)=\frac{\rho_3}{\rho_2}\frac{h_{30}}{\tau_{30}}(N^2_i+1)e^{(\Delta^2_i-\Delta^3_i)\bar{H}(\bar{X})}=\frac{h_{23}}{\tau_{23}}(N^2_i+1)e^{(\Delta^2_i-\Delta^3_i)\bar{H}(\bar{X})}$$

$$\Longleftrightarrow\ \boxed{R^i_{23}(\bar{X})=N^2_i\frac{h_{23}}{\tau_{23}}e^{(\Delta^2_i-\Delta^3_i)\bar{H}(\bar{X}-e^2_i)}}$$

$$\boxed{\bar{R}^i_{02}=\left[\frac{\rho_3}{\rho_0}\frac{h_{30}}{\tau_{30}}e^{-\Delta^3_i\bar{H}(\bar{X})}+\left(\frac{\rho_2}{\rho_0}\frac{h_{20}}{\tau_{20}}-\frac{\rho_1}{\rho_0}\frac{h_{12}}{\tau_{12}}\right)e^{-\Delta^2_i\bar{H}(\bar{X})}\right]N^0_i} \tag{3.17}$$

$$\boxed{\bar{R}^i_{01}=\frac{h_{01}}{\tau_{01}}N^0_i e^{-\Delta^1_i\bar{H}(\bar{X})}}$$

REMARK 3.1. The equal = sign to assign the new expression for the coarse grained rates $\bar{R}^i_{kl}$ in (3.9), (3.16), (3.17) is used for convenience although the main approximation will depend on the manner in which the coarse grained Hamiltonian will be constructed. This is performed next.

3.2. The coarse grained Hamiltonian and mean value approximation. It remains to compute appropriate approximate values for the potential differences

$$\bar{V}_{kl}(\bar{X},i):=\bar{H}_k(\bar{X},i)-\bar{H}_l(\bar{X},i),\ k,l=0,1,2,3,$$

to close the equations in (3.7). Here the convention $\bar{H}_0(\bar{X},i)=\bar{H}(\bar{X})$ is used. Let $\Delta^k\bar{H}(\bar{X},i)=\bar{H}(\bar{X}+e^k_i)-\bar{H}(\bar{X}),\ \ k=1,2,3,\ i=1,\cdots,M$. Then

$$\bar{V}_{kl}(\bar{X},i)=\Delta^k\bar{H}(\bar{X},i)-\Delta^l\bar{H}(\bar{X},i).$$

From the microscopic process, we have

$$\Delta^k H(X,j) = -\sum_{l=1}^{3} \sum_{r=1, r\neq j}^{N} J_{kl}(|r-j|) \mathbb{1}_{\{X^r=l\}}. \tag{3.18}$$

Let D_i be the coarse cell that contains the microscopic site j ($j \in D_i$). We derive an approximation $\Delta^k \bar{H}(\bar{X}, i)$ for $\Delta^k H(X,j)$ for all $j \in D_i$ following the main strategy used in [49, 50]. However, instead of using a Taylor expansion as Katsoulakis et al. [49, 50] did, here we use conditional expectation, as a rather exact estimation of the coarse grained potential differences. The Taylor approximation in [49, 50] is based on the long range interaction potential assumption and cannot be justified (at least in theory) for the case of nearest neighbour interactions. Other types of approximations were previously used for the short range interaction case but they require multi-body interactions [54].

Recall that the exact dynamics of the coarse grained process are given by the conditional expectation coarse grained rates in (3.7), that can be written generically as

$$\bar{R}^i_{kl} = E\left[\sum_{j \in D_i} R^j_{kl} \mathbb{1}_{\{X^j=k\}} / \bar{X}^i \right].$$

When the microscopic rates R^j_{kl} do not depend on X this expectation can be computed exactly without the knowledge of the conditional distribution of X given $\bar{X}$. In this case we have $\bar{R}^i_{kl} = R_{kl} N^k$. This is the case for the death rates in (3.9) and for all the transition rates in the case when local interactions were ignored [17].

Due to lack of knowledge, we assume that once the coarse process is fixed, the particles are "redistributed" uniformly within each coarse cell. This somewhat amounts to ignoring the effect of interactions across coarse cell interfaces on the distribution of particles within each coarse cell. More elaborate distributions that would take into account such interactions can be easily constructed but the present assumption is acceptable as a zeroth order approximation. Under such circumstances, the conditional distribution of X (within each coarse cell D_i) given the coarse grained process $\bar{X}^i = (N^i_1, N^i_2, N^i_3)$, $1 \le i \le M$, is that of a random variable consisting of randomly choosing a ball from an urn containing N^i_1 blue, N^i_2 yellow, N^i_3 red, and $N_0 = Q - N^i_1 - N^i_2 - N^i_3$ white balls, and these conditional expectations can be easily computed.

At each site $j \in D_i$, we have

$$P\{X_j = k\} = N_k/Q, \ k = 1,2,3 \text{ and } P\{X_j = 0\} = 1 - (N_1 + N_2 + N_3)/Q = \frac{N_0}{Q}.$$

For $j_1, j_2, \cdots, j_r \in D_i$, the joint distribution of $X_{j_1}, X_{j_2}, \cdots, X_{j_r}$ is a multinomial distribution corresponding to choosing r balls from an urn containing N^i_1 blue, N^i_2 yellow, N^i_3 red, and $N_0 = Q - N^i_1 - N^i_2 - N^i_3$ white balls.

Thus, the expectations in (3.7) can indeed be expressed exactly for any known interaction potentials J_{kl}. However, for the sake of simplicity we use the mean value approximation:

$$E\left[\sum_{j \in D_i} \tilde{R}_{kl} e^{(\Delta^k - \Delta^l) H(X,j)} \mathbb{1}_{\{X^j=k\}} / \bar{X}^i \right]$$

$$\approx e^{(\Delta^k-\Delta^l)E[H(X,j)/\bar{X},j\in D^i]}\times\sum_{j\in D_i}\tilde{R}_{kl}E[\mathbb{1}_{\{X^j=k\}}/\bar{X}]$$
$$=N_k\tilde{R}_{kl}e^{(\Delta^k-\Delta^l)E[H(X,j)/\bar{X},j\in D^i]}. \tag{3.19}$$

Although the exact analytical expression for the conditional expectations in (3.7) can be easily obtained, under the assumption of uniform conditional distribution (see Appendix A), the approximation in (3.19) is preferred and used here because, besides its computational simplicity, it preserves the Hamiltonian formulation of the process; It results in a coarse-grained Hamiltonian Markov process and a coarse-grained Gibbs canonical equilibrium measure. Nevertheless, the numerical tests performed in Section 5 demonstrate that the approximate-Hamiltonian coarse grained dynamics are qualitatively similar to the primitive microscopic process in terms of the time evolution of the cloud area fractions.

In fact, the approximation in (3.26) is equivalent to assuming the following definition/construction of the coarse-grained potential in (3.16) and (3.17), based on the conditional expectation:

$$\Delta^k\bar{H}(\bar{X},i)=E\left[\Delta^k H(X,j)/\bar{X},j\in D_i\right], \tag{3.20}$$

i.e, the coarse grained potential difference at coarse cell D_i is given by the conditional expectation of the corresponding microscopic potential difference at all sites $j\in D_i$ given the knowledge of $\bar{X}$.

Let n_b be the total number of interacting nearest neighbours of each microscopic site (figure 2.2). We assume n_b is constant. Let D_i be the coarse cell containing the site j and let $D_i^d, d=1,\cdots,n_b$ be the n_b neighbouring coarse cells of D_i. The expression for microscopic potential difference reduces as follows. We have for all $1\le k,l\le 3$,

$$\sum_{r=1,r\neq j}^{N}J_{kl}(|r-j|)\mathbb{1}_{\{X^r=l\}}=\sum_{r\in D_i,r\neq j}J_{kl}(|r-j|)\mathbb{1}_{\{X^r=l\}}+\sum_{d=1}^{n_b}\sum_{r\in D_i^d}J_{kl}(|r-j|)\mathbb{1}_{\{X^r=l\}}.$$

For each $j\in D_i$, we let G_j^k/i be the conditional expectation of $\Delta^k H(X,j)$ given $\bar{X}$ and given $j\in D_i$:

$$G^k_{j/i}=E[\Delta^k H(X,j)/\bar{X}^i,j\in D_i],$$

let D_i^s, D_i^e, D_i^n, D_i^w, D_i^{ne}, D_i^{nw}, D_i^{se}, and D_i^{sw} denote respectively the south, east, north, west, north-east, north-west, south-east, and south-west coarse cell neighbours of the cell D_i and let $\bar{X}^{ixy}$ be the value of the coarse process at the coarse cell D_i^{xy}. Then under the key assumption of uniform redistribution of particles inside each coarse cell, for fixed $\bar{X}_t$, we have

$$G^k_{j/i}=-\frac{1}{Q}\sum_{l=1}^{3}J^0_{kl}\times\begin{cases}n_bN_l^i, & \text{if } j\in\mathring{D}_i,\\ (n_b-n_b')N_l^i+n_b'N_l^{is}, & \text{if } j\in\partial\mathring{D}_i^s,\\ (n_b-n_b')N_l^i+n_b'N_l^{iw}, & \text{if } j\in\partial\mathring{D}_i^w,\\ (n_b-n_b')N_l^i+n_b'N_l^{in}, & \text{if } j\in\partial\mathring{D}_i^n,\\ (n_b-n_b')N_l^i+n_b'N_l^{ie}, & \text{if } j\in\partial\mathring{D}_i^e,\\ n_1N_l^i+n_2N_l^{is}+n_2N_l^{iw}+n_3N_l^{isw}, & \text{if } j\in\partial D_i^s\cap\partial D_i^w,\\ n_1N_l^i+n_2N_l^{in}+n_2N_l^{iw}+n_3N_l^{inw}, & \text{if } j\in\partial D_i^n\cap\partial D_i^w,\\ n_1N_l^i+n_2N_l^{is}+n_2N_l^{ie}+n_3N_l^{ise}, & \text{if } j\in\partial D_i^s\cap\partial D_i^e,\\ n_1N_l^i+n_2N_l^{in}+n_2N_l^{ie}+n_3N_l^{ine}, & \text{if } j\in\partial D_i^n\cap\partial D_i^e.\end{cases} \tag{3.21}$$

Here $\mathring{D}_i$ is the interior of the coarse cell D_i, i.e, all the microscopic sites within D_i which do not share an interface with a neighbouring coarse cell, $\partial\mathring{D}_i^x, x=n,s,e,w$ are the boundary alleys formed by sites of D_i that share an interface with the northern, southern, eastern, and western coarse cells, respectively, and $\partial D_i^x \cap \partial D_i^y, x\neq y$ represent the four corner sites of D_i (see figure 2.1). The coefficients n_b', n_1, n_2, and n_3 are defined in (3.22):

$$\begin{array}{ccccc} n_b & n_b' & n_1 & n_2 & n_3 \\ 4 & 1 & 2 & 1 & 0 \\ 8 & 3 & 3 & 2 & 1. \end{array} \tag{3.22}$$

Taking the expectation over j, we get for $q\geq 2$

$$\begin{aligned} &\Delta^k \bar{H}(\bar{X}) = E[G^k_{j/i}] \\ &= -\frac{1}{Q^2}\sum_{l=1}^{3} J^0_{kl}\left[\left(n_b(q-2)^2+4(n_b-n_b')(q-2)+4n_1\right)N_l^i\right. \\ &\quad \left.+\left(n_b'(q-2)+2n_2\right)\left(N_l^{is}+N_l^{in}+N_l^{ie}+N_l^{iw}\right)+n_3\left(N_l^{isw}+N_l^{ise}+N_l^{inw}+N_l^{ine}\right)\right]. \end{aligned} \tag{3.23}$$

Recall that $q=\sqrt{Q}$ is the resolution of the coarse cell. Note also that

$$\Delta_i^k \bar{H}(\bar{X}-\bar{e}_i^l) = \Delta_i^k \bar{H}(\bar{X}) + \frac{1}{Q^2}\left(n_b(q-2)^2+4(n_b-n_b')(q-2)+4n_1\right)J^0_{k,l}. \tag{3.24}$$

We note that despite the fact that (3.23) is derived for $q\geq 2$, it remains valid when $q=1$, in which case the coarse grained and the microscopic formulations are equivalent.

Equations (3.9), (3.16), (3.22), (3.23), and (3.24) completely determine the infinitesimal rates of an ergodic coarse grained process, for which the probability measure in (3.12) is the stationary distribution. It remains to express the coarse grained Hamiltonian.

According to the derivation above an expression for the coarse grained Hamiltonian is given by the conditional expectation given $\bar{X}$:

$$\bar{H}(\bar{X}) = E[H(X)/\bar{X}].$$

Thus

$$\bar{H}(\bar{X}) = \sum_{k=1}^{3}\sum_{l=1}^{3} E[E_{kl}(X)/\bar{X}] + \sum_{k=1}^{3} g_k(U)\sum_{i=1}^{M} N_k^i, \tag{3.25}$$

$$E[E_{kl}(X)/\bar{X}] = -\sum_{k=1}^{3}\sum_{j=1}^{N}\sum_{l=1}^{3}\sum_{r=1,r\neq j}^{N} E\left[J_{kl}(|j-r|)\mathbb{1}_{\{X^j=k\}}\mathbb{1}_{\{X^j=l\}}/\bar{X}\right]. \tag{3.26}$$

Again conditioning on $j\in D_i$, $1\leq j\leq N$, $1\leq i\leq M$ (with $N=QM$), we arrive at

$$\begin{aligned} &E[E_{kl}(X)/\bar{X}] \\ &= -\frac{1}{Q^2}\sum_{k=1}^{3}\sum_{l=1}^{3}\sum_{i=1}^{M} J^0_{kl}\left[\left(n_b(q-2)^2+4(n_b-n_b')(q-2)+4n_1\right)N_l^i\right. \end{aligned}$$

$$+(n_b'(q-2)+n_2)\left(N_l^{is}+N_l^{in}+N_l^{ie}+N_l^{iw}\right)+n_3\left(N_l^{isw}+N_l^{ise}+N_l^{inw}+N_l^{ine}\right)\Big]N_k^i, \tag{3.27}$$

which is consistent with (3.23). This completes the description of the coarse grained Hamiltonian. Interestingly, the coarse-grained Hamiltonian in (3.25)-(3.26) is identical to the one derived in [50] for one-type particle systems using Taylor expansions. This is not surprising at all since the Taylor expansion is performed based on the mean value on the coarse cell. However, the Taylor approximation procedure requires long range [49, 50] or multi-body interactions [54].

4. Equilibrium coverage and mean field equations

In equilibrium, the mean cloud coverage area fractions of congestus, deep, and stratiform clouds are given respectively by

$$\begin{aligned} E\sigma_c &= \frac{1}{N}\sum_{j=1}^{N} E[\mathbb{1}_{\{X^j=1\}}] = \frac{1}{N}\sum_{j=1}^{N}\text{Prob}\{X^j=1\},\\ E\sigma_d &= \frac{1}{N}\sum_{j=1}^{N} E[\mathbb{1}_{\{X^j=2\}}] = \frac{1}{N}\sum_{j=1}^{N}\text{Prob}\{X^j=2\},\\ E\sigma_s &= \frac{1}{N}\sum_{j=1}^{N} E[\mathbb{1}_{\{X^j=3\}}] = \frac{1}{N}\sum_{j=1}^{N}\text{Prob}\{X^j=3\}, \end{aligned} \tag{4.1}$$

$$\text{Prob}\{X^j=k\} = \sum_{x\in\Sigma, x^j=k} P(X=x) = \frac{1}{Z}\sum_{x\in\Sigma, x^j=k} P_N(X=x)e^{-H(x)},$$

where $Z=\sum_{\mathbf{x}\in\Sigma}P_N(X=\mathbf{x})\exp[-H(\mathbf{x})]$ and $P_N(X=\mathbf{x})=\prod_{r=1}^{N}\rho_{\mathbf{x}^r}$. When the local interactions are ignored, we have $\text{Prob}\{X^j=k\}=\rho_k$ and thus $E\sigma_c=\rho_1$, $E\sigma_d=\rho_2$, and $E\sigma_s=\rho_3$, but when local interactions are involved there is no obvious analytical formula for the probabilities in (4.1) and a brute force computation is nearly impossible; for a simple 10×10 lattice, the evaluation of Z alone involves the summation of about 10^{60} terms! Nevertheless, as shown by the numerical simulations below, the dynamical evolution of the stochastic process converges quickly to its statistical equilibrium and its running mean can be used to estimate the mean cloud area fractions. Another cheap way to obtain approximate values for the equilibrium area fractions is through the systematic derivation of the mean field equations, i.e, the differential equations satisfied by the expected values of the area fractions in (4.1), in the limit when the number of lattice sites is infinite. Formally, the mean field equations [48] are obtained by considering in (3.6) the family of test functions

$$\bar{f}_k^x(\bar{X}) = \frac{N_k^i}{Q} \quad \text{for} \quad x\in D_i,\ i=1,2,\cdots,M,\ k=1,2,3 \tag{4.2}$$

and taking the limit when both Q and M are infinitely large. This yields

$$\begin{aligned} \frac{\partial\sigma_1}{\partial t} &= \alpha_{01}\sigma_0-(\alpha_{10}+\alpha_{12})\sigma_1,\\ \frac{\partial\sigma_2}{\partial t} &= \alpha_{02}\sigma_0+\alpha_{12}\sigma_1-(\alpha_{20}+\alpha_{23})\sigma_2,\\ \frac{\partial\sigma_3}{\partial t} &= \alpha_{23}\sigma_2-\alpha_{30}\sigma_3. \end{aligned} \tag{4.3}$$

Here $\alpha_{kl}(x,t)\sigma_k$ is the formal limiting value of the infinitesimal rates $E[C(X,j,\eta)]$ in (2.5) where $x\in D_i$ and $\sigma_0=1-\sigma_1-\sigma_2-\sigma_3$, $\sigma_1=E\sigma_c$, $\sigma_2=E\sigma_d$, $\sigma_3=E\sigma_s$.

According to (2.17), we have

$$\alpha_{k0}=\tilde{R}_{k0}, k=1,2,3,\ \alpha_{01}=\tilde{R}_{01}e^{\Gamma_{10}},\ \alpha_{12}=\tilde{R}_{12}e^{\Gamma_{12}},\ \ \alpha_{23}=\tilde{R}_{23}e^{\Gamma_{23}},$$
$$\alpha_{02}=\frac{1}{\rho_0}(\rho_2\tilde{R}_{20}-\rho_1\tilde{R}_{12})e^{\Gamma_{20}}+\frac{\rho_3}{\rho_0}\tilde{R}_{30}e^{\Gamma_{30}}, \tag{4.4}$$

where [48]

$$\Gamma_{0k}(x)=\sum_{l=1}^{3}J_{kl}*\sigma_l(x) \text{ and } \Gamma_{kl}(x)=\Gamma_{0l}(x)-\Gamma_{0k}(x), \tag{4.5}$$

with $f*g(x)=\int f(x-y)g(y)\,dy$.

When solving the mean field equation (4.3) numerically the convolutions in (4.5) are approximated according to the quadrature formula [4]

$$\begin{aligned}J_{kl}*\sigma_l(x_1,x_2)\approx J^0_{kl}[&\sigma_l(x_1+\Delta x,x_2)+\sigma_l(x_1-\Delta x,x_2)\\&+\sigma_l(x_1,x_2+\Delta x)+\sigma_l(x_1,x_2-\Delta x)+\ \ \sigma_l(x_1+\Delta x,x_2+\Delta x)+\\&\sigma_l(x_1+\Delta x,x_2-\Delta x)+\sigma_l(x_1-\Delta x,x_2+\Delta x)+\sigma_l(x_1-\Delta x,x_2-\Delta x)]\end{aligned} \tag{4.6}$$

when $n_b=8$ and

$$\begin{aligned}J_{kl}*\sigma_l(x_1,x_2)\approx J^0_{kl}[&\sigma_l(x_1+\Delta x,x_2)+\sigma_l(x_1-\Delta x,x_2)\\&+\sigma_l(x_1,x_2+\Delta x)+\sigma_l(x_1,x_2-\Delta x)]\end{aligned} \tag{4.7}$$

when $n_b=4$. Here Δx is the numerical grid size and (x_1,x_2) is an arbitrary point of the grid.

5. Numerical tests

Here the microscopic and coarse-grained stochastic models and the mean field equations are solved numerically and their solutions are compared to each other in terms of the cloud-coverage area fractions. Both the cases with and without local interactions are considered. Recall that in the case without local interactions, $J_0=0$, the microscopic and coarse-grained processes yield the same exact solutions because the coarse grained rates are recovered exactly without any approximation.

To sample the stochastic models we use the exact algorithm of Gillespie [58, 59]. Given a configuration, X or $\bar{X}$, of respectively the microscopic or the coarse-grained stochastic process, the simulation algorithm consists in first finding the time at which the first transition occurs by simply taking a random sample of the exponential distribution whose rate is the sum of the rates of all the possible transitions, and then a second random sample determines which or these transitions actually occurs. The mean field equation (4.3) is integrated by the Matlab routine ODE45 on a 10×10 grid.

Unless otherwise stated all the simulations use the standard parameters listed in Table 5.1. We note that most of these parameters (including the time scales) are not physically realistic. They are picked arbitrarily just for the sake of illustration. More realistic time scales, for the case without local interaction, can be found in the disciplinary publications [45, 46] and especially in [47] where the stochastic multicloud model is calibrated and assessed against observations.

In figure 5.1, two realizations of the stochastic multicloud lattice model, (a) with and (b) without ($J_0 = 0$) local interactions are displayed. As we can see from figure 5.1, one of the main differences from the local interactions and non local interaction models is that local interactions allow self-organization of convection into coherent patches. While in figure 5.1(b) the distribution of cloud types within the lattice appear to be completely random, figure 5.1(a) show a different picture. It is characterized by the clustering (especially, of congestus and deep) cloud states to form distinct and persistent patches. Due to the largest coefficient of congestus-congestus interaction in the interaction matrix in Table 5.1 congestus patches are more prominent and consistently seconded by deep convective patches. We note that 40×40 sites are used in figure 5.1 for a better illustration.

$\tau_{10} = 5$ hours	$\tau_{20} = 5$ hours	$\tau_{30} = 5$ hours
$\tau_{12} = 2$ hours	$\tau_{01} = 2$ hours	$\tau_{02} = 2$ hours
$\tau_{23} = 3$ hours		
$C = 0.25$	Convection potential	
$D = 0.5$	Tropospheric dryness	
$h_{10} = \Gamma(D)/\tau_{10}$	$h_{20} = (1-\Gamma(C))/\tau_{20}$	$h_{30} = 1/\tau_{30}$
$h_{12} = \Gamma(C)(1-\Gamma(D))/\tau_{12}$	$h_{23} = \Gamma(C)/\tau_{23}$	$h_{01} = \Gamma(D)\Gamma(C)/\tau_{01}$
$h_{02} = (1-\Gamma(D))\Gamma(C)/\tau_{02}$		
$\Gamma(x) = 1 - e^{-x}$	if $x > 0$,	0 otherwise
J_0	Interaction matrix	$\begin{bmatrix} 0.25 & 0 & 0 \\ 0 & 0.125 & 0.05 \\ 0 & 0.05 & 0.125 \end{bmatrix}$
$n = 20$	$q = 10$	$n_b = 8$

TABLE 5.1. *List of parameter values used in the numerical simulations. See [17] for physical meanings.*

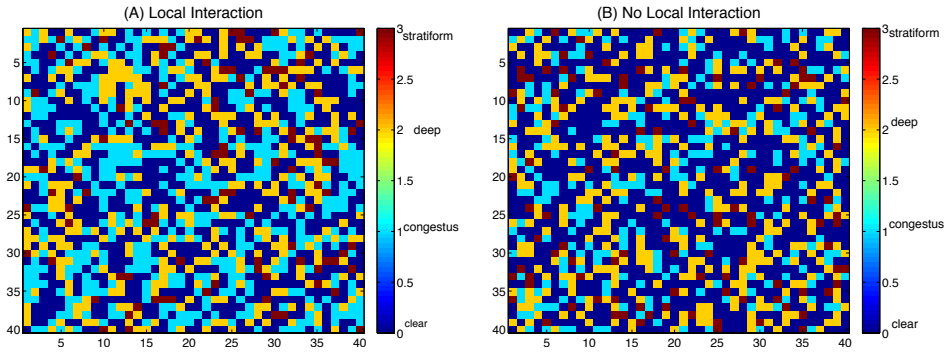

FIG. 5.1. *Snapshot of the multicloud microscopic lattice model. (a) With local interactions and (b) without local interactions.* $n = 40$.

In figure 5.2, we plot the time evolution of the cloud coverage for the case of local interactions using (a) the microscopic model and (b) the coarse grained process and (c) for the case of non local interactions $J_0 = 0$ [17] for the parameter values listed in Table 5.1. All the simulations are run for a total time period of 10 days starting from

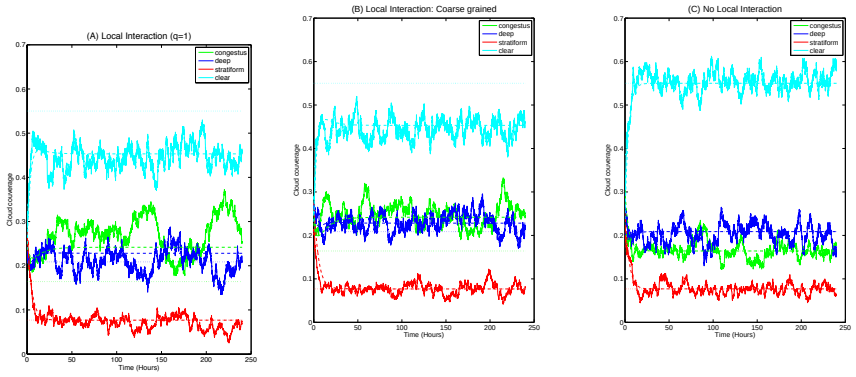

FIG. 5.2. *Time evolution of cloud area fractions for the case of local interactions using (a) the microscopic lattice model and (b) the coarse grained process and (c) for the case without local interactions. Solid: stochastic process, Dashes: mean field equation, Dots: prior distribution.*

n,q	Model	σ_c	σ_d	σ_s
	MF	0.24179	0.22822	0.076831
$n=10,\ q=1$	Micro	0.27398	0.21947	0.069977
$n=10,\ q=5$	GC	0.23681	0.22037	0.084618
$n=10,q=10$	GC	0.24038	0.23089	0.076733
$n=20,\ q=1$	Micro	0.27634	0.21613	0.072294
$n=20,q=5$	GC	0.24018	0.225	0.077071
$n=20,q=10$	GC	0.24766	0.23021	0.077164
$n=20,q=20$	GC	0.25271	0.21896	0.080075
$n=40,q=1$	Micro	0.2576	0.22589	0.072762
$n=40,q=10$	GC	0.2394	0.22703	0.077575
$n=40,q=20$	GC	0.23521964	0.23386534	0.07783689

TABLE 5.2. *Time averaged cloud area fraction for the stochastic and mean field models with local interactions. The mean is based on a 10 days simulation and computed over the last 7.5 days of the simulation to discard the transient.*

random initial data. Recall that in the latter case the microscopic and coarse grained models are equivalent. In each case, the stochastic time series are plotted on top of the corresponding deterministic solution of the mean field equations in (4.3), the dashed lines. A common feature for all the stochastic time series is that after a short transient period they quickly converge to their statistical equilibrium and then undergo chaotic variability oscillations of significant amplitude around their corresponding statistical means. The mean field equations on the other hand converge monotonically to their equilibrium values and stay locked there forever.

The dotted lines in figure 5.2 correspond to the background prior distribution values. As expected while in the case without local interactions in figure 5.2(c) this corresponds to mean field limit, significant deviations from the prior are noticeable due to local interactions. Various numeral tests (not shown here) demonstrate that as the strength of local interactions is increased these deviations become more and more important. A too strong $J^0_{1,1}$ value for example yields an equilibrium value locked at

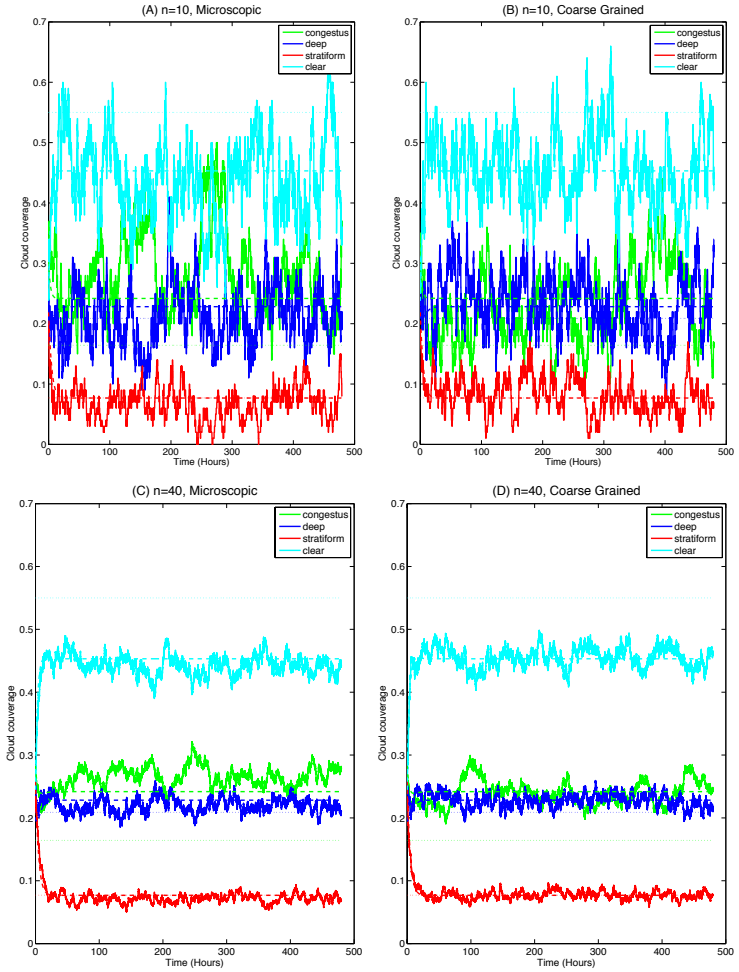

FIG. 5.3. *Same as figure 5.2(a) and (b) but for* $n = 10, 40$.

all sites being congestus and has a very weak variability.

While in the case of non-local interactions the stochastic time series oscillate around the associated mean field equilibrium values, the local interactions time series appear to have a time average slightly off the corresponding mean field values, especially in the case of the microscopic process ($q = 1$); the congestus time series in figure 5.2(a) for example oscillate above the mean field limit and is characterized by very long excursions biased towards the accumulation of congestus, consistent with the persistence of the congestus patches seen in figure 5.1. Importantly, the same behaviour is also observed in the case of the coarse grained solution in figure 5.2(b) but the excursions are slightly short lived and they seem to occur equally in both directions. Indeed, from the formal derivation of the mean field equations in Section 4, convergence to the mean field limit occurs when both q and n are infinitely large. This is somewhat corroborated by the results in table 5 where the time average of the stochastic time series corresponding to the local interaction case are calculated and

compared against the mean field limit for various values of q and n; see also the plots in figure 5.3.

While a systematic mathematical investigation of the convergence issue is desirable, the goal of this work is to develop a coarse grained stochastic model which is intermediate between the microscopic lattice model with multi-type interacting particles and its mean field limit for the case of local interactions as a physically improved version of the stochastic multicloud of Khouider et al. [17].

6. Conclusion

A coarse graining methodology for multi-type particle interacting systems on a lattice is developed here in the context of tropical convection. The aim is to provide a systematic way to include local interactions between lattice sites as an extension to the stochastic multicloud model of Khouider et al. [17]. The lattice system takes values 0, 1, 2, and 3 at each single site according to whether the given site is clear sky or occupied by congestus, deep, or stratiform cloud types.

The coarse grained strategy employed here follows the framework of Katsoulakis et al. [49, 50], developed in the context of the one-type particle interacting system best known as the Ising model. The main methodology consists in overlying a coarse lattice on top of the fine-microscopic lattice and define a new order parameter that counts the number of lattice sites that are occupied by each type of clouds within each coarse cell. This results in a multidimensional birth-death process with immigration whose transition rates are given by the conditional expectations of the sums of the microscopic transition rates over each coarse cell. When the effect of interactions across coarse cells on the redistribution of particles with the coarse cells are ignored, the associated conditional probability mass function is simply the multinomial distribution which permits in principle an easy integration of these expectation given the microscopic interaction potentials. While under such an assumption the exact expectations can be obtained in closed form, here a mean value approximation is adopted in order to obtain approximate coarse rates that are in semi-detailed balance with respect to a coarse grained Gibbs canonical measure and a coarse grained Hamiltonian, which is used as a design principle. This is different from the Taylor approximation method used in [49] which relies on the assumption of a long range interaction potential or the approximation used in [54] which requires multi-body interactions. Nearest neighbour interactions are more relevant for the tropical convection application mainly because all the physical mechanisms through which cloud types can interact locally, besides the large scale conditions, such as gravity waves, turbulent mixing, density currents, etc., have a finite speed of propagation.

Numerical tests performed in Section 5 demonstrate that despite this crude approximation the coarse grained model captures the main stochastic variability of the original microscopic model in terms of the total area coverage, i.e, the cloud fractions. Moreover, the coarse grained process shows consistently a tendency to converge to the mean field equations when both the number of coarse cell and the number of microscopic sites are large.

The nearest neighbour interactions are represented by an interaction matrix whose entries can be set arbitrarily according to the application and thus the model can be easily adopted to other situations even if the number of particle types is augmented or reduced. To augment the portability, both the situations of 4 and 8 nearest neighbours are considered. However, for the case of tropical convection considered here, for example, these entries are very uncertain. Nevertheless, they could be inferred from detailed numerical simulations or from in situ measurements of clouds using well

known statistical techniques such as Bayesian inference of parameters and the like. Such methodologies are being developed by the author and various collaborators for the background time scales τ_{kl} in (2.15). They can be easily extended to include the interaction matrix coefficients into the picture, although this will considerably increase the dimensionality of the parameter system, from 7 to 16. However, in theory, physical intuition can be used to set up values for this matrix (as we did in Section 5) in order to gain some understanding about the effect of local interactions on the behaviour of the stochastic multicloud parameterization when coupled to a climate model [17, 45, 46].

Acknowledgment. This research is supported by the Natural Science and Engineering Council of Canada. The author would like to thank Andrew Majda and Markos Katsoulakis for helpful discussion. Part of this work is accomplished at NYU Abu Dhabi when the author was on a long visit to the Center for Prototype Climate Models in January 2013.

Appendix A. Exact coarse grained rates. As stated above, the exact analytical expression of the coarse-grained rates (3.7) can be easily obtained through simple algebraic manipulations. This is illustrated here for the case of the birth rates $\bar{R}^i_{0k}$, $k=1,2$. According to (3.7)

$$\bar{R}^i_{0k} = \sum_{j\in D_i} E[R^j_{0k}\mathbb{1}_{\{X^j=0\}}/\bar{X}^i].$$

We have

$$\begin{aligned} R^i_{0k} &= \tilde{R}_{0k}e^{-\Delta^k H(X,j)} = \tilde{R}_{0k}\exp\left[\sum_{l=1}^{3}\sum_{r=1,r\neq j}^{N} J_{kl}(|r-j|)\mathbb{1}_{\{X^r=l\}}\right] \\ &= \tilde{R}_{0k}\prod_{l=1}^{3}\prod_{r=1,\neq j}^{N}\exp\left[J_{kl}(|r-j|)\mathbb{1}_{\{X^r=l\}}\right]. \end{aligned} \tag{A.1}$$

For $j\in D_i$, let

$$m^j_k = E\left[\mathbb{1}_{\{X^j=0\}}\prod_{l=1}^{3}\prod_{r=1,\neq j}^{N}\exp\left[J_{kl}(|r-j|)\mathbb{1}_{\{X^r=l\}}\right]\right].$$

We assume that once the coarse variables are set, the particles are uniformly distributed within each coarse cell. This amounts to ignoring the effect of the interactions across coarse cells on the local redistribution of particles (see text). Then, with the nearest neighbour potential assumption and when all the neighbouring cells are within D^i, the probability mass function related to this conditional expectation is that of choosing s_b blue, s_y yellow, s_r red, and $n_b+1-s_b-s_y-s_r$ white balls, $0\le s_b+s_y+s_r\le n_b$, from an urn containing containing N_1 blue, N_2 yellow, N_3 red and $N_0=Q-N_1-N_2-N_3$ white balls (a multivariate hyper-geometric random variable). Thus for $j\in\mathring{D}^i$ we have

$$m^j_k := \mathring{m}^j_k = \sum_{0\le s_b+s_y+s_r\le n_b} P^i_{s_b,s_y,s_r}\exp\left[s_bJ^0_{k1}+s_yJ^0_{k2}+s_rJ^0_{k3}\right],$$

where

$$P^i_{s_b,s_y,s_r} = \binom{N_1^i}{s_b}\binom{N_2^i}{s_y}\binom{N_3^i}{s_r}\binom{N_0^i}{n_b+1-s_b-s_y-s_r}\Big/\binom{Q}{n_b+1}.$$

(There are $(q-2)^2$ such interior points $j \in D^i$.) Similar formulae can be derived for lattice sites near the boundary and a closed form for the expectations in (A.1) can be obtained. The remaining details are a simple exercise of probability theory.

The errors associated with the mean value approximation can also, in principle, be estimated in terms of the conditional variance of the microscopic potentials $\Delta^k H(X,j)$ given $\bar{X}$, which can also be easily expressed in terms of the coarse-grained process. We have for the birth rates, for example,

$$\begin{aligned} E\left[\left|\bar{R}_{0k} - \bar{R}^{mv}_{0k}\right|^2/\bar{X}\right] &= \left(N_0\tilde{R}_{0k}\right)^2 E\left[\left(\exp\left(-\Delta^k H(X,j)\right) - \exp\left(-\Delta^k \bar{H}(\bar{X})\right)\right)^2/\bar{X}\right] \\ &\approx \left(N_0\tilde{R}_{0k}\right)^2 \mathrm{Var}\left[\Delta^k H(X,j)/\bar{X}\right], \end{aligned}$$

where the superscript mv refers to the mean value approximation.

REFERENCES

[1] T.M. Liggett, *Stochastic Interacting Systems: Contact, Voter and Exclusion Processes*, Grundlehren der Mathematischen Wissenschaften, Springer, Berlin, 324, 1999.

[2] C. Thompson, *Mathematical Statistical Mechanics*, Princeton Univ. Press, Princeton, 1972.

[3] G. Giacomin and J.L. Lebowitz, *Phase segregation dynamics in particle systems with long range interactions. i. Macroscopic limits*, J. Stat. Phys., 87–137, 1997.

[4] A.J. Majda and B. Khouider, *Stochastic and mesoscopic models for tropical convection*, Proc. Nat. Acad. Sci., 99, 1123–1128, 2002.

[5] B. Khouider, A. Majda, and M. Katsoulakis, *Coarse grained stochastic models for tropical convection and climate*, Proc. Nat. Acad. Sci., 100, 11941–11946, 2003.

[6] A.J. Majda, C. Franzke, and B. Khouider, *An applied mathematics perspective on stochastic modelling for climate*, Phil. Trans. Roy. Soc. A: Math., Phys. Engin. Sci., 366(1875), 2427–2453, 2008.

[7] D.G. Vlachos, *The role of macroscopic transport phenomena in film microstructure during epitaxial growth*, Appl. Phys. Lett., 74, 2797–2799, 1999.

[8] D.G. Vlachos and M.A. Katsoulakis, *Derivation and validation of mesoscopic theories for diffusion-reaction of interacting molecules*, Phys. Rev. Lett., 85(18), 3898–3901, 2000.

[9] M.A. Katsoulakis and P.E. Souganidis, *Stochastic Ising models and anisotropic front propagation*, J. Stat. Phys., 87, 63–89, 1997.

[10] N. Dundon and A. Sopasakis, *Stochastic modeling and simulation of multi-lane traffic*, Transport. Traffic Theory, 661–691, 2006.

[11] A. Sopasakis and M.A. Katsoulakis, *Stochastic modeling and simulation of traffic flow: Asep with Arrhenius look-ahead dynamics*, SIAM J. Appl. Math., 66, 921–944, 2006.

[12] M.A. Katsoulakis, A.J. Majda, and A. Sopasakis, *Multiscale couplings in prototype hybrid deterministic/stochastic systems: Part i, Deterministic closures*, Commun. Math. Sci., 2(2), 255–294, 2004.

[13] M.A. Katsoulakis, A.J. Majda, and A. Sopasakis, *Multiscale couplings in prototype hybrid deterministic/stochastic systems: Part ii, Stochastic closures*, Commun. Math. Sci., 3(3), 453–478, 2005.

[14] M.A. Katsoulakis, A.J. Majda, and A. Sopasakis, *Hybrid deterministic stochastic systems with microscopic look-ahead dynamics*, Commun. Math. Sci., 8(2), 409–437, 2010.

[15] A. Chatterjee and D.G. Vlachos, *Continuum mesoscopic framework for multiple interacting species and processes on multiple site types and/or crystallographic planes*, J. Chem. Phys., 127, 034705, 2007.

[16] V. Spyratos, P. Bourgeron, and M. Ghil, *Development at the wildland-urban interface and the mitigation of forest-fire risk*, Proc. Natl. Acad. Sci. USA, 104, 14272–14276, 2007.

[17] B. Khouider, J. Biello, and A.J. Majda, *A stochastic multicloud model for tropical convection*, Commun. Math. Sci., 8(1), 187–216, 2010.

[18] A. Chertock, A. Kurganov, A. Polizzi, and I. Timofeyev, *Pedestrian flow models with slowdown interactions*, Math. Models Meth. Appl. Sci., 24, 249, 2014.
[19] J.-L. Lin, G.N. Kiladis, B.E. Mapes, K.M. Weickmann, K.R. Sperber, W. Lin, M.C. Wheeler, S.D. Schubert, A. Del Genio, L.J. Donner, S. Emori, J.-F. Gueremy, F. Hourdin, P.J. Rasch, E. Roeckner, and J.F. Scinocca, *Tropical intraseasonal variability in 14 IPCC AR4 climate models. Part I: Convective signals*, J. Climate, 19(12), 2665–2690, 2006.
[20] M.W. Moncrieff and E. Klinker, *Organized convective systems in the tropical western Pacific as a process in general circulation models: A TOGA COARE case-study*, Quart. J. Roy. Meteor. Soc., 123, 805–827, 1997.
[21] J.M. Slingo, K.R. Sperber, J.S. Boyle, J.P. Ceron, M. Dix, B. Dugas, W. Ebisuzaki, J. Fyfe, D. Gregory, J.F. Gueremy, J. Hack, A. Harzallah, P. Inness, A. Kitoh, W. K.-M. Lau, B. McAvaney, R. Madden, A. Matthews, T.N. Palmer, C.K. Parkas, D. Randall, and N. Renno, *Intraseasonal oscillations in 15 atmospheric general circulation models: Results from an AMIP diagnostic subproject*, Climate Dynamics, 12, 325–357, 1996.
[22] M.W. Moncrieff, M. Shapiro, J. Slingo, and F. Molteni, *Collaborative research at the intersection of weather and climate*, WMO Bulletin, 56, 204–211, 2007.
[23] P. Ray and C. Zhang, *A case study of the mechanics of extratropical influence on the initiation of the Madden-Julian Oscillation*, J. Atmos. Sci., 67, 515–528, 2010.
[24] B. Liebmann and D. Hartmann, *An observational study of tropical-midlatitude interaction on intraseasonal time scales during winter*, J. Atmos. Sci., 41, 3333–3350, 1984.
[25] H. Lin, G. Brunet, and J. Derome, *An observed connection between the North Atlantic Oscillation and the Madden-Julian Oscillation*, J. Climate, 22, 364–380, 2009.
[26] A. Arakawa, *The cumulus parameterization problem: Past, present, and future*, J. Climate, 17, 2493–2525, 2004.
[27] R.H. Johnson, T.M. Rickenbach, S.A. Rutledge, P.E. Ciesielski, and W.H. Schubert, *Trimodal characteristics of tropical convection*, J. Climate, 12(8), 2397–2418, 1999.
[28] G.N. Kiladis, M.C. Wheeler, P.T. Haertel, K.H. Straub, and P.E. Roundy, *Convectively coupled equatorial waves*, Rev. Geophys., 47, RG2003, doi:10.1029/2008RG000266, 2009.
[29] B. Khouider and A.J. Majda, *A simple multicloud parametrization for convectively coupled tropical waves. Part I: Linear analysis*, J. Atmos. Sci., 63, 1308–1323, 2006.
[30] B. Khouider and A.J. Majda, *Multicloud models for organized tropical convection: Enhanced congestus heating*, J. Atmos. Sci., 65, 897–914, 2008.
[31] B. Khouider and A.J. Majda, *Equatorial convectively coupled waves in a simple multicloud model*, J. Atmos. Sci., 65, 3376–3397, 2008.
[32] B. Khouider and A.J. Majda, *Multicloud convective parametrizations with crude vertical structure*, Theor. Comput. Fluid Dyn., 20, 351–375, 2006.
[33] A.J. Majda, S. Stechmann, and B. Khouider, *Madden-Julian Oscillation analog and intraseasonal variability in a multicloud model above the equator*, Proc. Nat. Acad. Sci., 104, 9919–9924, 2007.
[34] B. Khouider, Y. Han, A. Majda, and S. Stechmann, *Multi-scale waves in an MJO background and CMT feedback*, J. Atmos. Sci., 69, 915–933, 2012.
[35] B. Khouider, A. St-Cyr, A.J. Majda, and J. Tribbia, *The MJO and convectively coupled waves in a coarse-resolution GCM with a simple multicloud parameterization*, J. Atmos. Sci., 68(2), 240–264, 2011.
[36] B. Khouider, A. Majda, and S. Stechmann, *Climate science in the tropics: Waves, vortices and PDEs*, Nonlinearity, 26, R1–R68, 2013.
[37] R. Buizza, M. Miller, and T.N. Palmer, *Stochastic representation of model uncertainties in the ECMWF Ensemble Prediction System*, Quart. J. Roy. Meteor. Soc., 125, 2887–2908, 1999.
[38] J.W.B. Lin and J.D. Neelin, *Influence of a stochastic moist convective parameterization on tropical climate variability*, Geophys. Res. Lett., 27, 3691–3694, 2000.
[39] J. Lin and J. Neelin, *Toward stochastic deep convective parameterization in general circulation models*, Geophys. Res. Lett., 30, 1162, 2003.
[40] R. Plant and G. Craig, *A stochastic parameterization for deep convection based on equilibrium statistics*, J. Atmos. Sci., 65, 87–105, 2008.
[41] T.N. Palmer, *A nonlinear dynamical perspective on model error: A proposal for non-local stochastic-dynamic parametrization in weather and climate prediction models*, Quart. J. Roy. Meteor. Soc., 127, 279–304, 2001.
[42] S.N. Stechmann and J.D. Neelin, *A stochastic model for the transition to strong convection*, J. Atmos. Sci., 68, 2955–2970, 2011.
[43] I. Horenko, *Nonstationarity in multifactor models of discrete jump processes, memory and application to cloud modeling*, J. Atmos. Sci., 68, 1493–1506, 2011.
[44] A.J. Majda and S.N. Stechmann, *A simple dynamical model with features of convective mo-*

mentum transport, J. Atmos. Sci., 66, 373–392, 2009.
[45] Y. Frenkel, A.J. Majda, and B. Khouider, *Using the stochastic multicloud model to improve tropical convective parameterization: A paradigm example*, J. Atmos. Sci., 69(3), 1080–1105, 2012.
[46] Y. Frenkel, A.J. Majda, and B. Khouider, *Stochastic and deterministic multicloud parameterizations for tropical convection*, Climate Dyn., 41, 1527–1551, 2013.
[47] K. Peters, C. Jakob, L. Davies, B. Khouider, and A. Majda, *Stochastic behaviour of tropical convection in observations and a multicloud model*, J. Atmos. Sci., 70, 3556–3575, 2013.
[48] D.J. Horntrop, M.A. Katsoulakis, and D.G. Vlachos, *Spectral methods for mesoscopic models of pattern formation*, J. Comput. Phys., 173, 364–390, 2001.
[49] M.A. Katsoulakis, A.J. Majda, and D.G. Vlachos, *Coarse-grained stochastic processes for microscopic lattice systems*, Proc. Nat. Acad. Sci. U.S.A., 100(3), 782–787, 2003.
[50] M.A. Katsoulakis, A.J. Majda, and D.G. Vlachos, *Coarse-grained stochastic processes and Monte Carlo simulations in lattice systems*, J. Comput. Phys., 186(1), 250–278, 2003.
[51] M.A. Katsoulakis, P. Plechac, and A. Sopasakis, *Error control and analysis in coarse-graining for stochastic lattice dynamics*, SIAM J. Numer. Anal., 4(6), 2270–2296, 2006.
[52] A. Chatterjee and D.G. Vlachos, *Multiscale spatial Monte Carlo simulations: Multigriding, coarse-graining schemes for short and long-range interactions computational singular perturbation, and hierarchical stochastic closures*, J. Chem. Phys., 124, 064110, 2006.
[53] J. Dai, W.D. Seider, and T. Sinno, *Coarse-grained lattice kinetic Monte Carlo simulation of systems of strongly interacting particles*, J. Chem. Phys., 128, 194705, 2007.
[54] S. Are, M.A. Katsoulakis, P. Plecháč, and L. Rey-Bellet, *Multibody interactions in coarse-graining schemes for extended systems*, SIAM J. Sci. Comput., 31, 987–1015, 2008.
[55] B. Mapes, S. Tulich, J. Lin, and P. Zuidema, *The mesoscale convection life cycle: Building block or prototype for large-scale tropical waves?* Dyn. Atmos. Oceans, 42(1–4), 3–29, 2006.
[56] S. Ross, *Introduction to Probability Models*, Ninth Edition, Academic Press, 2007.
[57] E. Renshaw, *Modelling Biological Populations in Space and Time*, Cambridge Studies in Mathematical Biology, Cambridge University Press, 1993.
[58] D.T. Gillespie, *An exact method for numerically simulating the stochastic coalescence process in a cloud*, J. Atmos. Sci., 32, 1977–1989, 1975.
[59] D.T. Gillespie, *Exact stochastic simulation of coupled chemical reactions*, The J. Phys. Chem., 81(25), 2340–2361, 1977.